



**HAL**  
open science

## **Bisphenols disrupt differentiation of the pigmented cells during larval brain formation in the ascidian**

Isa D.L. Gomes, Ievgeniia Gazo, Dalileh Nabi, Lydia Besnardeau, Céline Hebras, Alex Mcdougall, Rémi Dumollard

### ► To cite this version:

Isa D.L. Gomes, Ievgeniia Gazo, Dalileh Nabi, Lydia Besnardeau, Céline Hebras, et al.. Bisphenols disrupt differentiation of the pigmented cells during larval brain formation in the ascidian. *Aquatic Toxicology*, 2019, 216, pp.105314. 10.1016/j.aquatox.2019.105314 . hal-02362929

**HAL Id: hal-02362929**

**<https://hal.science/hal-02362929>**

Submitted on 21 Dec 2021

**HAL** is a multi-disciplinary open access archive for the deposit and dissemination of scientific research documents, whether they are published or not. The documents may come from teaching and research institutions in France or abroad, or from public or private research centers.

L'archive ouverte pluridisciplinaire **HAL**, est destinée au dépôt et à la diffusion de documents scientifiques de niveau recherche, publiés ou non, émanant des établissements d'enseignement et de recherche français ou étrangers, des laboratoires publics ou privés.



Distributed under a Creative Commons Attribution - NonCommercial 4.0 International License

# 1 Bisphenols disrupt differentiation of the pigmented cells during 2 larval brain formation in the ascidian

3  
4  
5 Isa D.L. Gomes<sup>a,\*</sup>, Ievgeniia Gazo<sup>a,b</sup>, Dalileh Nabi<sup>a#</sup>, Lydia Besnardeau<sup>a</sup>, Céline Hebras<sup>a</sup>,  
6 Alex McDougall<sup>a</sup>, Rémi Dumollard<sup>a,\*</sup>

7  
8 <sup>a</sup>Laboratoire de Biologie du Développement de Villefranche-sur-mer (LBDV) UMR7009, Sorbonne Universités,  
9 Université Pierre-et-Marie-Curie, CNRS, Institut de la Mer de Villefranche (IMEV), Villefranche-sur-mer,  
10 France

11 <sup>b</sup>University of South Bohemia in Ceske Budejovice, Faculty of Fisheries and Protection of Waters, Research  
12 Institute of Fish Culture and Hydrobiology, Laboratory of Molecular, Cellular and Quantitative Genetics, Zátíší  
13 728/II, 389 25, Vodňany, Czech Republic

14  
15 \* Corresponding authors: [remi.dumollard@obs-vlfr.fr](mailto:remi.dumollard@obs-vlfr.fr); [igobio12@gmail.com](mailto:igobio12@gmail.com)

16 # Current address: Medical Theoretical Center, TU-Dresden, Fiedlerstrasse 42, D-01307 18 Dresden,  
17 Germany

---

## 21 Abstract

22  
23 The endocrine disruptor Bisphenol A (BPA), a widely employed molecule in plastics, has been shown to  
24 affect several biological processes in vertebrates, mostly via binding to nuclear receptors.  
25 Neurodevelopmental effects of BPA have been documented in vertebrates and linked to neurodevelopmental  
26 disorders, probably because some nuclear receptors are present in the vertebrate brain. Similarly, endocrine  
27 disruptors have been shown to affect neurodevelopment in marine invertebrates such as ascidians, mollusks or  
28 echinoderms, but whether invertebrate nuclear receptors are involved in the mode-of-action is largely unknown.

29 In this study, we assessed the effect of BPA on larval brain development of the ascidian *Phallusia*  
30 *mammillata*. We found that BPA is toxic to *P. mammillata* embryos in a dose-dependent manner (EC<sub>50</sub>:  
31 11.8µM; LC<sub>50</sub>: 21µM). Furthermore, micromolar doses of BPA impaired differentiation of the ascidian  
32 pigmented cells, by inhibiting otolith movement within the sensory vesicle. We further show that this phenotype  
33 is specific to other two bisphenols (BPE and BPF) over a bisphenyl (2,2 DPP). Because in vertebrates the  
34 estrogen-related receptor gamma (ERRγ) can bind bisphenols with high affinity but not bisphenyls, we tested  
35 whether the ascidian ERR participates in the neurodevelopmental phenotype induced by BPA. Interestingly, *P.*  
36 *mammillata* ERR is expressed in the larval brain, adjacent to the differentiating otolith. Furthermore,  
37 antagonists of vertebrate ERRs also inhibited the otolith movement but not pigmentation. Together our  
38 observations suggest that BPA may affect ascidian otolith differentiation by altering *Pm*-ERR activity whereas  
39 otolith pigmentation defects might be due to the known inhibitory effect of bisphenols on tyrosinase enzymatic  
40 activity.

## 41 Keywords:

42  
43  
44  
45 Ascidian, Bisphenol A, Estrogen-related receptor, Invertebrate, Neurodevelopment, Otolith

## 46 Abbreviations:

47  
48 BPA: bisphenol A; DES: diethylstilbestrol; ED: endocrine disruptor; ERR: estrogen-related receptor; E2B: 17β-  
49 estradiol 3-benzoate; NR: nuclear receptor; PC: pigmented cells; 4OHT: 4-hydroxytamoxifen

## 51 **1. Introduction**

52 Bisphenol A (BPA), a well-known molecule used in plastics, was considered harmless to human health until  
53 Krishnan and colleagues found that it could easily leach from plastics into their yeast cultures (Krishnan et al.  
54 1993). BPA was later found accidentally to be a potent meiotic aneugen in mouse females (Hunt et al. 2003).  
55 Because BPA is continuously released into the environment, human and wildlife are ubiquitously exposed  
56 despite its short half-life, making BPA a pseudo-persistent chemical (Flint et al. 2012). Consequently,  
57 concerns have been raised about BPA due to its potential endocrine disrupting activities. Endocrine disruptors  
58 (EDs) are compounds able to mimic hormones and interfere with different biological processes (Gomes et al.  
59 2019; Schug et al. 2016).

60 In vertebrates, BPA has several targets such as membrane receptors like G protein-coupled estrogen  
61 receptor 1 (GPER), the aryl hydrocarbon receptor (AhR), or several nuclear receptors such as Estrogen  
62 Receptor (ER), Estrogen-Related Receptor (ERR), Peroxisome Proliferator-Activated Receptor (PPAR),  
63 Pregnane X Receptor (PXR) and Thyroid Receptor (TR) (Delfosse et al. 2014; Acconcia et al. 2015; Murata  
64 and Kang 2017; Mackay and Abizaid 2018). While disruption of steroid and thyroid systems by EDs have been  
65 associated with the presence of nuclear receptors in the reproductive system and thyroid (ER, AR, TR), the  
66 discovery of nuclear receptors presence in the vertebrate brain (ER, ERR, PPAR and PXR) lead researchers  
67 to suspect about the potential hazard of EDs to vertebrate neurodevelopment and to link these chemicals with  
68 an increase of neurodevelopmental disorders (Inadera 2015; Mustieles et al. 2015; Braun 2017; Nesan et al.  
69 2017).

70 Previous reviews have shown that invertebrate development can also be affected by BPA (Flint et al. 2012;  
71 Canesi and Fabbri 2015; Dumollard et al. 2017). Studies indicate that BPA may be harmful to wildlife even at  
72 environmentally relevant concentrations (0.05 $\mu$ M or lower) (Flint et al. 2012). The highest concentration found  
73 in natural surface waters was 0.1 $\mu$ M, but landfill leachates from municipal wastes registered BPA  
74 concentrations around 75 $\mu$ M (Flint et al. 2012). Even though the toxicity of BPA has been described and  
75 studied in invertebrates, there is a lack of knowledge concerning its mode-of-action, including BPA's impact on  
76 neurodevelopment (Kaur et al. 2015; Mersha et al. 2015; Dumollard et al. 2017; Messinetti et al. 2018a;  
77 Messinetti et al. 2018b). Because invertebrate embryos do not possess a circulatory system (transporting  
78 hormones), nuclear receptors are the most likely targets for endocrine disruption as they are found in all  
79 marine invertebrates, from marine sponges to ascidians (Holzer et al. 2017). Yet, roles of most nuclear  
80 receptors (NRs) in invertebrates are still poorly known and efforts are being made to fill this gap (Gomes et al.  
81 2019; Markov and Laudet 2011; Holzer et al. 2017). Unlike vertebrates, other mechanisms of toxicity  
82 (membrane receptors, oxidative stress, epigenetics) are completely unknown in invertebrates and they are not  
83 as conserved as NR signaling is (Gomes et al. 2019; Holzer et al. 2017).

84 Ascidians (Tunicata) are marine invertebrate chordates. Upon fertilization, the ascidian embryo develops  
85 into a larva that shows a prototypical chordate body plan (Hudson 2016) within only 18 hours (Hotta et al.  
86 2007). The brain of the ascidian larva is located in the trunk and is composed by an anterior sensory vesicle  
87 and a trunk ganglion (Gomes et al. 2019), and expresses typical specification markers such as *Cnga*, *Coe*,  
88 *Islet*, *Pax6*, among others (Hudson 2016). In the sensory vesicle, two pigmented cells (PC) are visible, the  
89 otolith and the ocellus. The otolith (Ot), responsible for gravity sensing, is an unicellular structure which has a  
90 free part within the lumen of the sensory vesicle and a ventral foot part (Dilly 1962; Esposito et al. 2015). The  
91 ocellus (Oc), involved in light perception, was previously described as a multicellular structure made up of one  
92 pigmented cell, three lens cells and 37 photoreceptor cells (Dilly 1964; Ryan et al. 2016). Specification  
93 process of the PC starts at late gastrula (stage 13) by the induction of specific genes such as tyrosinase (*Tyr*),  
94 tyrosinase-related proteins (*Tyrp1/2a*, *Tyrp1/2b*) and the GTPase *Rab32/38* (Nishida and Satoh 1989;  
95 Racioppi et al. 2014). At late neurula (st. 16), PC specification ends and differentiation starts. While the gene  
96 regulatory network (GRN) involved in ascidian PC specification is well characterized, the GRN involved in PC  
97 differentiation is not known. Recent studies in ascidians showed that BPA affects neurodevelopment by  
98 disrupting the pigmented cells and GABAergic and dopaminergic neurons, and it was even suggested that the  
99 ascidian nuclear receptor ERR might be involved in the toxic mode-of-action of BPA (Messinetti et al. 2018b;  
100 Messinetti et al. 2018a). Nevertheless, phenotype of BPA on ascidian PC is still poorly characterized and the  
101 presence of ERR in the ascidian embryo is currently unknown.

102 In this study, we assessed the effect of BPA on brain development of the ascidian larva (*Phallusia*  
103 *mammillata*). By imaging PC behavior and analyzing gene expression in the forming ascidian brain, we found  
104 that BPA at lower doses specifically impairs PC development by disrupting otolith pigmentation and  
105 differentiation. We further show that this phenotype is also induced by bisphenol E and bisphenol F but not by  
106 a bisphenyl or estradiol. Because in vertebrates ERRγ has been shown to bind bisphenols but not bisphenyls,  
107 and due to previous reports on ERR implication in zebrafish otolith development (Tohmé et al. 2014), we  
108 decided to test if the ascidian ERR could be mediating BPA toxicity. We found that *P. mammillata* ERR is  
109 expressed in the ascidian sensory vesicle during PC differentiation and ERR antagonists partially copied BPA  
110 phenotype, suggesting that it might participate in the neurodevelopmental effect of BPA in the ascidian larva.

## 111 **2. Material and Methods**

### 112 **2.1. Animals**

113 *Phallusia mammillata* adults were collected in Sète (Hérault, France), and kept at 17±1°C in circulating  
114 seawater aquaria. They were reared under constant light conditions to avoid uncontrolled spawning of eggs  
115 and sperm (Lambert and Brandt, 1967). The animals were kept and maintained by the *Centre de Ressources*  
116 *Biologiques Marines* of the institute (CRBM - IMEV).

117 For exposure experiments, eggs and sperm were collected separately by dissecting the gonoducts of  
118 several hermaphrodite adults. Sperm was stored at 4°C, while eggs were placed in natural filtered (0.2 µm)  
119 seawater (FSW) supplemented with TAPS buffer (0.5 mM) and EDTA (0.1 mM) (Sardet et al. 2011). To allow  
120 fluorescence microscopy analysis, chorion was removed from eggs by incubating in a trypsin solution for 2  
121 hours, and then washed 3 times before use (McDougall et al. 2015). Eggs were fertilized by incubating them  
122 with a sperm dilution (1:100) for 10 min, then washed 3 times and left in filtered seawater (FSW/TAPS/EDTA)  
123 at 18°C until the desired developmental stage. Since *Phallusia mammillata* development is very similar to  
124 *Ciona robusta*, all referred developmental stages are based on published *Ciona* development (Hotta et al.  
125 2007). Please refer to figure 2D for general ascidian developmental stages and figure 2A for specific brain  
126 developmental stages. The details of all protocols for embryos handling can be found online at [http://lbdv.obs-  
128 vlfr.fr/fr/ascidian-biocell-group.html](http://lbdv.obs-<br/>127 vlfr.fr/fr/ascidian-biocell-group.html) .

### 129 **2.2. Chemical products**

130 For embryo culture, TAPS buffer (CAS Nr. 29915-38-6) and EDTA (CAS Nr. 60-00-4) were used. For  
131 toxicity studies, the following chemicals were diluted in dimethyl sulfoxide (DMSO, CAS Nr. 67-68-5):  
132 Bisphenol A (BPA, CAS Nr. 80-05-7), Bisphenol E (BPE, CAS Nr 2081-08-5), Bisphenol F (BPF, CAS Nr 620-  
133 92-8), Diethylstilbestrol (DES, CAS Nr 56-53-1), Phenylthiourea (PTU, CAS Nr. 103-85-5), UO126 (CAS Nr.  
134 109511-58-2), β-Estradiol 3-benzoate (E2B, CAS Nr 50-50-0), 2,2-Diphenylpropane (2,2DPP, CAS Nr 778-22-  
135 3), 4-Hydroxytamoxifen (4OHT, CAS Nr 68392-35-8). For F-actin and DNA staining, phalloidin-  
136 tetramethylrhodamine B isothiocyanate (Phalloidin-TRITC, Santa Cruz Biotechnology) and Hoechst (CAS Nr.  
137 23491-52-3) were used, and samples conserved with Citifluor AF1 antifade mounting solution (Biovalley). All  
138 chemicals were purchased from Sigma Aldrich, unless stated otherwise.

### 139 **2.3. Exposure experiments**

140 Exposure experiments with BPA, BPE, BPF, 2,2 DPP, E2B, DES, 4OHT and PTU were performed in the  
141 same way. Chemicals were dissolved in DMSO to have a 0.5 M main stock solution. After fertilization, stage 1  
142 embryos were transferred to chemical-containing seawater (FSW-TAPS-EDTA). Due to a possible confusion  
143 arising from differences in the concentrations of DMSO, each solution was diluted in DMSO to a concentration  
144 10,000 times higher than required, and again diluted in filtered seawater (1:10000), giving the required  
145 concentration of chemical in an overall solution of 0.01% DMSO in seawater. As a control treatment, 0.01%  
146 DMSO seawater was used.

147 For the exposure experiment with UO126, the chemical was dissolved in a 0.04 M DMSO stock solution.  
148 Embryos were fertilized and left to develop at 18°C until stage 16. Embryos were then exposed at stages 16  
149 and 18, at a final concentration of 4 µM defined from a previous study (Racioppi et al. 2014). A control  
150 treatment with 0.01% DMSO was performed.

153 At stage 26, larvae were fixed in 4% paraformaldehyde (4% PFA, 0.5 M NaCl, PBS; Sigma), washed 3  
154 times in Phosphate Buffered Saline (PBS 1X) and imaged by light microscopy (*Zeiss Axiovert 200*) at 10x  
155 magnification. Each experiment was replicated at least 3 times.

156

#### 157 **2.4. Embryo morphology analysis**

158 For general morphology analysis, larvae (st. 26) were analyzed by scoring the percentage of normal (good  
159 general embryo morphology, with proper trunk and palps formation, as well as tail elongation), malformed  
160 (embryos with bent tail) and not developed embryos (with arrested development before gastrulation/tail  
161 extension) (see figure 1). Statistical analysis was performed as described in section 2.11.

162 For trunk morphology analysis, the area of each PC (*PC area*,  $\mu\text{m}^2$ ), the distance between the two PCs (*PC*  
163 *distance*,  $\mu\text{m}$ ) and the length and width of the trunk were measured and transformed in a ratio (Trunk L/W  
164 ratio) (see figure 2A). The morphological analysis was performed using *Toxicosis*, a software developed in our  
165 laboratory (*IDDN.FR.001.330013.000.S.P.2018.000.10000*, deposited on July 13th 2018). The resulting data  
166 was normalized to each respective control treatment (100%) and plotted in radar charts for better comparison  
167 of phenotypes between chemicals. Statistical analysis was performed as described in section 2.11. Please  
168 note that only exposure experiments with control treatments showing a mean PC area equal or superior to 300  
169  $\mu\text{m}^2$  and a percentage of undeveloped embryos lower than 20% were suitable for further analysis.

170

#### 171 **2.5. BPA time-window action**

172 To assess the time-window action of BPA during *Phallusia mammillata* embryogenesis, embryos were  
173 incubated in BPA-containing seawater at different times during embryogenesis. In a first phase, embryos were  
174 exposed in three different ways: 1) six hours before fertilization (6 *hbf*), 2) six hours after fertilization (6  
175 *hpf*, time to reach gastrulation, i.e. stage 10), or 3) both before and after fertilization (from stage 0 to 10) for a total  
176 of 12 hours BPA exposure (please refer to diagram on figure 2D). Embryos were then washed and incubated  
177 in FSW/TAPS/EDTA up to stage 26. In a second phase, embryos were exposed at different stages (10, 12,  
178 14, 16, 18 and 20) until stage 26. At stage 26, embryos from all treatments were fixed (4% PFA) for later  
179 analysis of pigment cell area (*PC area*,  $\mu\text{m}^2$ ). For a matter of technical feasibility, embryos were cultured at  
180 14°C from fertilization to stage 16 and then placed at 18°C from stage 16 to stage 26. Statistical analysis was  
181 performed as described in section 2.11.

182

#### 183 **2.6. Immunofluorescence**

184 To assess the effect of BPA on mitotic spindle formation, microtubule organization during the first mitosis  
185 was assessed. For this, eggs were fertilized and immediately exposed to 0.01% DMSO or BPA 40  $\mu\text{M}$ . Sixty-  
186 four minutes after fertilization (during the first mitosis), embryos were fixed in cold 100% methanol overnight.  
187 They were then progressively rehydrated in PBS/0.02% Triton, permeabilized in PBS/0.25% Triton for 15 min at  
188 RT, and then incubated in primary and secondary antibodies in PBS/1% BSA overnight at 4°C (for each  
189 antibody incubation, fixed embryos were washed for 15 min for 4 times with PBS/0.1% Tween). Fixed embryos  
190 were stained for microtubules with primary antibody anti- $\alpha$ -tubulin (DM1A; Sigma-Aldrich 1:1000) and mouse  
191 FITC secondary antibody (Jackson) diluted 1:50. To stain DNA, immunofluorescence labelled embryos were  
192 mounted in VectaShield that contains DAPI (Vector Laboratories) analyzed with epifluorescence microscopy  
193 (40X objective, *Zeiss Axiovert 200*).

194 Cilia in the neurohypophysial duct and neural tube were assessed by immunostaining with anti-acetylated  
195  $\alpha$ -tubulin antibody according to previously published protocols (Sardet et al. 2011). Stained larvae were  
196 imaged by confocal microscopy (Leica, SP8).

197

#### 198 **2.7. Analysis of otolith movement by timelapse imaging**

199 To follow otolith development, eggs were injected with reporter plasmids bearing promoter region for *Ciona*  
200 genes driving the expression of GFP based reporters. The promoters used are Tyrosinase-related protein  
201 (pTyrp, kind gift from Filomena Ristatore),  $\beta\gamma$ Crystallin (p $\beta\gamma$ C, kind gift from Philip Abitua) and Muscle  
202 segment homeobox (pMsx, kind gift from Philip Abitua) to visualize pigment cell precursors. The GFP-based  
203 reporters were either Venus/Cherry (cytosolic), H2B::Venus/Cherry (DNA) or Lifeact::Venus/Cherry (actin-rich  
204 cell cortex). To visualize the plasma membrane of all cells mRNAs coding for PHdomain::Tomato was injected

205 in unfertilized eggs as previously described (McDougall et al. 2015). Injected eggs were fertilized 2 hours after  
206 injection and left to develop until stage 10 (gastrula). Then, embryos were either transferred to 0.01% DMSO  
207 (figure 3A) or to BPA-containing seawater (10  $\mu$ M, figure 3B) and at stage 20 (early tailbud) embryos were  
208 mounted on a slide for time-lapse live imaging using confocal microscopy (Leica SP8).  
209

## 210 **2.8. Analysis of otolith foot by Phalloidin staining**

211 To analyze the otolith foot structure, embryos were exposed to BPA analogues BPE, BPF and 2,2 DPP  
212 (section 2.3). Once at the desired stage (st. 26), embryos were fixed with 4% PFA overnight at 4°C. Embryos  
213 were washed twice with PBS 1X, incubated in PBS-BSA solution (3% BSA diluted in PBS 1X) for 1h and  
214 stained with Phalloidin-TRITC and Hoechst diluted 1:500 in PBS-BSA, for 3h at RT. Embryos were washed  
215 twice in PBS-BSA, once in PBS and stored in AF1 antifade mounting solution Citifluor (Biovalley) until  
216 analysis. Phenotypes were compared to a control treatment (0.01% DMSO) using confocal microscopy (Leica  
217 SP8). Please note the same final concentration was used for all molecules (10 $\mu$ M), with the exception of  
218 2,2DPP (25 $\mu$ M), since no phenotype was visible at 10 $\mu$ M, 25 $\mu$ M nor 100 $\mu$ M.  
219

## 220 **2.9. mRNA expression pattern analysis by *in situ* hybridization (ISH)**

221 mRNA expression patterns of *Phallusia mammillata* genes were assessed by *in situ* hybridization (ISH)  
222 technique. For this, embryos were fixed overnight at 4°C (ISH fix: 4% formaldehyde, 100 mM MOPS, 0.5 M  
223 NaCl, pH 7.6), washed in PBS, dehydrated in ethanol and stored at -20°C until analysis. *Phallusia* ISH was  
224 performed as previously described (Paix et al. 2009).

225 ISH probes covering the entire cDNAs were designed based on *Aniseed* (<http://www.aniseed.cnrs.fr/>) and  
226 *Octopus* (<http://octopus.obs-vlfr.fr/index.php>) databases and were obtained from the *Phallusia mammillata*  
227 cDNA library (pExpress-1 vector based) available in our laboratory. After amplification by PCR and  
228 confirmation by electrophoresis, PCR products were purified (Qiagen MinElute PCR purification kit, Qiagen)  
229 and DNA quantified. Digoxigenin-labeled antisense RNA probes (DIG RNA Labeling Mix, Roche) were then  
230 prepared and detection was based on NBT/BCIP (Roche) principle. The following genes were assessed: Tyr  
231 (gene ID: *Phamm.g00005364*), Rab32/38 (gene ID: *Phamm.g00006935*), Pax6 (gene ID:  
232 *Phamm.g00010911*), Cnga (gene ID: *Phamm.g00015101*), Coe (gene ID: *Phamm.g00012706*) and Islet (gene  
233 ID: *Phamm.g00000576*). The imaging of all embryos was performed using bright field microscopy (*Zeiss*  
234 *Axiovert 200*).  
235

## 236 **2.10. Estrogen-Related Receptor embryonic expression**

237 The sequence for *Phallusia mammillata* ERR (*Pm-ERR*) is published on *Aniseed* database (gene ID:  
238 *Phamm.g00012306*) and was cloned from *Phallusia mammillata* cDNA library and processed by ISH as  
239 described in section 2.9.  
240

### 241 2.10.1. *Pm-ERR* gene activity by promoter cloning

242 Gene activity was assessed by cloning the promoter region of *Pm-ERR* into a vector driving the expression  
243 of a GFP reporter. For this, a 1.7 kbp fragment (-1705 from the Transcription Start Site, *TSS*, figure 6C) was  
244 selected from ascidian genome available on *Aniseed* database. This region, which is highly conserved with  
245 *Phallusia fumigata*, was amplified by PCR from *P. mammillata* genomic DNA and cloned upstream a  
246 H2B::Venus reporter by In-Fusion HD Cloning Plus kit (Takara Bio). The prepared construct  
247 (pERR>H2B::Venus) was microinjected in *P. mammillata* eggs and the transgenic embryos analyzed by  
248 confocal imaging (Leica TCS SP8).  
249

### 250 2.10.2. *Pm-ERR* protein levels analyzed by a specific antibody against *Pm-ERR*

251 To determine protein presence by immunoblot, an antibody against the ERR protein was made by  
252 producing the protein and sending it to Covalab (France) to immunize mice. Four anti-serum were screened  
253 and results from the most reactive anti-serum are shown. The anti-serum was further validated as described in  
254 figure 6D. In order to confirm the antibody specificity, the antibody was tested against exogenous *Pm-ERR*  
255 (*Pm-ERR*::Venus mRNA injected larvae).  
256

## 257 **2.11. Statistical analysis**

258 All presented data show mean with error bars indicating standard deviation (mean±SD). The number of  
259 embryos (*n*) analyzed for each graph is indicated in the figure legend. For figure 2C and figure 6, descriptive  
260 statistics is depicted in table I. For figure 2D, *n* and *P* values are indicated in the figure legend.

261 GraphPad Prism® software (GraphPad Software, Inc. CA, USA) was used to calculate median lethal (LC<sub>50</sub>)  
262 and effective (EC<sub>50</sub>) concentrations, as well as to perform analysis of variance ( $\alpha=0,05$ ) to evaluate differences  
263 between treatments. Since data did not follow a Gaussian distribution (Shapiro-Wilk normality test),  
264 nonparametric Kruskal-Wallis test was performed and statistical differences between control and treatments  
265 were assessed by Dunnett's test.

266

## 267 **3. Results**

### 268 **3.1. Bisphenol A is toxic to *P. mammillata* embryos in a dose-dependent manner**

269 Figure 1 shows the effect of BPA on the general morphology of *Phallusia* embryos after 24 hours of  
270 exposure. Embryos of *P. mammillata* were exposed to different concentrations of BPA (from 100 nM to 30  $\mu$ M)  
271 and a significant increase in malformed and not developed larvae was observed from 10  $\mu$ M BPA (compared  
272 to the control treatment 0.01% DMSO, ANOVA - Dunnett's Multiple Comparison Test:  $p<0.05$ , figure 1). At 15  
273  $\mu$ M and 20  $\mu$ M larvae were mostly malformed (60% and 65%, respectively), and at 25 and 30  $\mu$ M larvae were  
274 mostly not developed (95% and 100%, respectively). Observation of the mitotic spindle in one cell embryos  
275 exposed to 40  $\mu$ M BPA showed a severe disruption of mitotic spindle in BPA exposed embryos compared to  
276 controls (fig S1) suggesting that at this dose BPA acts as an aneugenic genotoxic. No visible effect was  
277 detected when embryos were exposed to nanomolar concentrations. BPA median effective (EC<sub>50</sub>, malformed)  
278 and lethal (LC<sub>50</sub>, not developed) concentrations for *P. mammillata* embryogenesis were 11.8  $\mu$ M and 21  $\mu$ M,  
279 respectively.

280

### 281 **3.2. Bisphenol A induces neurodevelopmental toxicity in *P. mammillata* embryos**

282 Careful observation revealed that at 10  $\mu$ M of BPA, within embryos showing normal overall morphology  
283 with proper trunk and tail elongation (figure 1), the pigmented cells (PC) within the sensory vesicle were  
284 strongly affected. In order to better describe the phenotype of BPA, formation of sensory vesicle was recorded  
285 by timelapse imaging of embryonic development between stage 21 (early tailbud) and stage 26 (hatching  
286 larva) (figure 2A, 2B), during which differentiation of the sensory vesicle and pigmented cells occurs (Esposito  
287 et al. 2015).

288 In non-exposed embryos (0.01% DMSO, figure 2A), the first pigments appear at stage 21 (black  
289 arrowhead), increasing at stage 22. At stage 23 adhesive palps start to protrude (yellow arrowhead) and two  
290 distinct PC are visible: the ocellus (*Oc*, blue arrowhead) and the otolith (*Ot*, pink arrowhead). At this stage, a  
291 lumen is first visible in the sensory vesicle (orange arrowhead) and this lumen expands until stage 26. At stage  
292 25, the trunk begins to elongate and concomitantly the otolith moves towards the ventral side of the sensory  
293 vesicle. Finally, at stage 26, larvae display two clearly separated PC and palps, as well as an elongated trunk.  
294 Note that pigmentation, otolith movement and other events happen concomitantly.

295 When comparing to non-exposed embryos, embryos exposed to BPA at stage 1 (BPA 10  $\mu$ M) clearly  
296 showed a reduction of pigmentation and a blocked otolith movement towards the ventral side of the sensory  
297 vesicle (figure 2B). Additionally, both sensory vesicle lumen (svl) formation and trunk elongation seemed  
298 slightly reduced. Palps were the only well-formed structures when compared to non-exposed embryos. We  
299 then quantified pigmentation by measuring the area of both PC (PC area); the otolith movement by measuring  
300 the distance between PC (PC distance); and the trunk by measuring the length and width (Trunk L/W ratio).  
301 BPA-exposed embryos showed significant reduction for all the three endpoints (ANOVA - Dunnett's Multiple  
302 Comparison Test:  $p$ -value<0.001; table I), with PC area reduced to 35%, PC distance reduced to 31%  
303 whereas Trunk L/W ratio was less affected (reduced to 70%) (figure 2C). Additionally, the sensory vesicle  
304 lumen seemed also reduced but this was not quantified.

305 In order to understand the window of action of BPA on pigmented cells formation, embryos were incubated  
306 at different times during embryogenesis (figure 2D). Reduction of pigmentation (PC area) was always  
307 observed when BPA was present between stage 10 and stage 26 (ANOVA - Dunnett's Multiple Comparison  
308 Test:  $p$ -value<0.001), and not when it was washed before stage 10. Strikingly, reduced pigmentation was still

309 observed when BPA was added as late as stage 20. We also exposed eggs to BPA before fertilization (stages  
310 0-1 and 0-10) to assess whether bioaccumulation of BPA could influence the phenotypes observed. However,  
311 even when BPA was allowed to accumulate for 6-12 hours and washed out at stage 10, no effect on  
312 pigmentation was observed.

313 In *Ciona*, the formation of the pigmented cells necessitates tyrosinase activity for the pigmentation of  
314 melanosomes (Caracciolo et al. 1997) and FGF/MAPK signals up to stage 16 for specification (Racioppi et al.  
315 2014). Accordingly, *Phallusia* embryos exposed to the tyrosinase enzyme inhibitor phenylthiourea (PTU, from  
316 1-cell stage (Whittaker 1966; Sakurai et al. 2004)) resulted in the complete lack of pigmented melanosomes in  
317 the PC, but the unpigmented otolith cell seemed well formed and ventrally placed in the sensory vesicle lumen  
318 (figure S2A). The phenotype obtained is clearly different from the phenotype induced by application of BPA at  
319 a similar timing (figure 2B).

320 Moreover, embryos exposed to the MAPK inhibitor UO126 at stage 16 are completely devoid of PC and  
321 sensory vesicle lumen, whereas embryos treated with UO126 at stage 18 display two well separated PC and  
322 normal sensory vesicle lumen (figure S2A). Once again, the phenotypes induced by MAPK inhibition are  
323 different from the observed BPA phenotype. In addition, spatial expression of *Tyr*, *Rab32/38*, *Pax6*, *Cnga*, *Coe*  
324 and *Islet* genes, known to be necessary for PC and/or CNS specification, was analyzed by *in situ* hybridization  
325 (ISH) (figure S2B). No differences in the spatial expression patterns between non-exposed (DMSO) and BPA-  
326 exposed embryos (BPA 10 $\mu$ M) were observed, suggesting that BPA does not affect PC nor CNS specification.  
327 Finally, differentiation of the neurohypophysial duct and neural tube (Konno et al. 2010) was not affected by  
328 BPA as shown in figure S2C, reinforcing the idea that only PC differentiation is affected by BPA exposure.

329

### 330 **3.3. Bisphenol A impairs otolith cell movement towards the ventral side of the sensory vesicle**

331 We have observed so far that BPA affects processes intervening in sensory vesicle differentiation between  
332 stage 21 and 26. In order to characterize with more precision, we performed time-lapse imaging of embryos  
333 expressing fluorescent-tagged reporters in the pigmented cells (PC) lineage. By using the otolith specific  
334 promoter (*p $\beta$ YC::GFP*) we could clearly observe changes in the shape of the otolith between stage 21 (when it  
335 is in the epithelium of the sensory vesicle) and stage 25 (when the otolith is bulging into the sensory vesicle  
336 lumen and contacts the sensory vesicle epithelium by a foot structure) (figure 3A). The actin network of PC  
337 was specifically visualized with a PC specific promoter (*pTyrp>LifeAct::3xVenus*) together with bright field  
338 imaging. Timelapse imaging shows that the otolith cell detaches its foot from the dorsal sensory vesicle  
339 epithelium (and from the ocellus) at stage 26, moving towards the ventral side of the sensory vesicle  
340 epithelium (figure 3B and supplementary movie 1). Note that the sensory vesicle lumen also expands during  
341 these stages. In BPA-exposed embryos, the otolith cell still forms its foot but it does not detach from the dorsal  
342 sensory vesicle epithelium, remaining tethered to the ocellus. In addition, expansion of the sensory vesicle  
343 lumen seems to be reduced (figure 3C and supplementary movie 2).

344 We then assessed whether this phenotype is specific to bisphenol A, by exposing embryos to BPE and  
345 BPF (two other bisphenols) and 2,2DDP (a bisphenyl) (figure 4A). For this, exposed larvae (stage 26) were  
346 stained with Phalloidin and Hoechst to visualize both actin and DNA structures. The control larvae (0.01%  
347 DMSO, figure 4B) showed an accumulation of actin abutting the otolith foot on the ventral side of the sensory  
348 vesicle. In contrast BPA-exposed larvae displayed a dorsal/posterior otolith actin-rich foot (figure 4C).  
349 Interestingly, both BPE and BPF exposures resulted in the presence of the otolith actin-rich foot in the dorsal  
350 side of the sensory vesicle (figures 4D and 4E), suggesting that otolith movement did not occur. Finally,  
351 exposure to 25 $\mu$ M 2,2 DPP did not affect the localization of the otolith foot which was still observed on the  
352 ventral side of the sensory vesicle (figure 4F), suggesting that the bisphenyl does not affect otolith movement.  
353 No phenotype was observed with either 10 or 100 $\mu$ M 2,2 DPP (data not shown). Even though we did not  
354 quantify it, BPE and BPF (but not 2,2 DPP) also seem to decrease PC pigmentation and sensory vesicle  
355 lumen expansion (compare the different larvae shown in figures 4B-F). Because bisphenols but not bisphenyl  
356 have been previously shown to bind human Estrogen-Related Receptor (ERR) with high affinity (see  
357 Discussion), we thus sought for ERR presence in *P. mammillata* larvae.

358

### 359 **3.4. Estrogen-Related Receptor (ERR) is expressed in *Phallusia mammillata* larvae**

360 In order to substantiate the possibility that BPA targets ERR in the ascidian embryo, we analyzed ERR  
361 transcripts and protein level during embryonic development (figure 5). Published transcriptomic data in the  
362 ascidian *Aniseed* database suggests that ERR transcripts are found at larvae (stage 26) but not before  
363 (Gomes et al. 2019). ISH analysis revealed that, at stage 26, ERR is expressed within the sensory vesicle,  
364 more precisely above the ocellus, between otolith and ocellus and underneath the otolith, as well as in  
365 adhesive palps and trunk ganglion (figure 5A, black arrowheads). Since ISH staining using NBT/BCIP at such  
366 a late stage is made difficult by the secretion of the ascidian tunic (larvae become dark quickly), we further  
367 confirmed ERR zygotic expression by monitoring its promoter activity (pERR>H2B::Venus) in transgenic  
368 embryos (Stolfi and Christiaen 2012) (figure 5B). On the 20 injected larvae, all showed fluorescent nuclei (i.e.  
369 promoter activity) in the sensory vesicle, with 13 having additional cells in the adhesive palps, while the other 7  
370 had additional cells in the trunk ganglion. Additionally, 2 larvae showed ectopic expression in the mesenchyme  
371 due to promoter leakiness previously reported in ascidians (Stolfi and Christiaen 2012).

372 Using an antibody specific for *Pm*-ERR (figure 5C), ERR protein levels were measured during development  
373 by western blot analysis (figure 5D). As expected from transcriptomic data available from the ascidian  
374 database *Aniseed*, ISH and promoter analysis, a strong band ( $\approx$  50 kDa) was observed at stage 26 but not  
375 before.

376

### 377 **3.5. ERR antagonists also affect PC development**

378 BPA is known to bind both ER $\alpha$  and ER $\beta$  and also ERR $\gamma$  in vertebrates (Takayanagi et al. 2006). We thus  
379 exposed embryos to the ER agonist  $\beta$ -Estradiol 3-benzoate (E2B) and to the ERR antagonists  
380 diethylstilbestrol (DES) and 4-hydroxytamoxifen (4OHT). These ERR antagonists were selected as they have  
381 been shown to inhibit ERR from another ascidian species (*Halocynthia roretzi*) by transactivation assays in a  
382 human cell line (Park et al. 2009). Effect of E2B, DES and 4OHT on PC differentiation and trunk elongation  
383 was assessed. Figure 6 shows radar chart plotting of the relative differences in three measured endpoints (PC  
384 area, PC distance and Trunk L/W ratio) between control and exposed embryos, in order to compare the  
385 phenotypes induced by the different molecules.

386 As expected (see Discussion), the ER agonist E2B did not affect any endpoint measured (figure 6A, table  
387 I). Regarding PC differentiation, the PC distance was significantly reduced by both ERR antagonists, although  
388 to a lesser extent than BPA (figures 2C, 6B and 6C; table I; BPA 10 $\mu$ M: 31%, DES 1 $\mu$ M: 65%, 4OHT 10 $\mu$ M:  
389 58%). The trunk elongation was also affected in similar proportions with BPA (figures 2C, 6B and 6C; table I;  
390 BPA 10 $\mu$ M: 70%, DES 1 $\mu$ M: 75%, 4OHT 10 $\mu$ M: 75%). Finally, PC area was not significantly affected by DES  
391 (figure 6B and table I; DES 1 $\mu$ M: 101%) nor by 4OHT (figure 6C and table I; 4OHT 5 $\mu$ M: 98%, 10 $\mu$ M: 105%),  
392 contrarily to BPA (figure 2C and table I; BPA 10 $\mu$ M: 35%). Please note that the concentration of DES used  
393 (1 $\mu$ M) was relatively low compared to BPA or 4OHT (5 $\mu$ M-10 $\mu$ M) due to the fact that embryos showed high  
394 sensitivity to DES (100% undeveloped embryos at 2 $\mu$ M, data not shown).

395 Our pharmacological screen shows that ERR antagonists can partially reproduce the phenotype of BPA, by  
396 affecting the PC distance, i.e., the otolith movement within the sensory vesicle, but not the pigmentation  
397 process.

398

## 399 **4. Discussion**

400 BPA has been shown to affect multiple targets and may have diverse and pleiotropic modes-of-action.  
401 Moreover, embryonic development has been shown to be one of the most critical windows of action for EDCs,  
402 particularly during neurodevelopment (Heyer and Meredith 2017). In our study we show that BPA acts during a  
403 precise window of the ascidian embryonic development, disrupts the pigmentation process and specifically  
404 blocks otolith movement within the sensory vesicle. A pharmacological approach suggests that the observed  
405 phenotype may be specific to bisphenols (BPE, BPF) over a bisphenyl (2,2 DPP). Finally, we hypothesize that  
406 the effect of BPA on ascidian larval brain formation may be mediated by ERR as suggested by a screen of  
407 ERR antagonists and the zygotic expression of ERR in a few cells of the sensory vesicle.

408

### 409 **4.1. Bisphenol A is toxic to ascidian embryos**

410 *Phallusia mammillata* embryos display a dose-dependent sensitivity to BPA with a common monotonic  
411 dose-response curve. Moreover, in our study BPA was shown to affect *P. mammillata* pigmented cells, in a  
412 similar way as recently published (Messinetti et al. 2018a), as well as in another ascidian species, *Ciona*  
413 *robusta* (Matsushima et al. 2013; Messinetti et al. 2018b). However, because of variability of the neural  
414 phenotypes reported before (Messinetti et al. 2018a), we performed a quantitative analysis of brain formation  
415 to better define BPA phenotype.

416 Concerning dose-response toxicity, our data indicates that *P. mammillata* embryos are less sensitive to  
417 BPA (EC<sub>50</sub>: 11.8µM; LC<sub>50</sub>: 21µM) than other marine invertebrates like the ascidian *Ciona robusta* (EC<sub>50</sub>:  
418 0.7µM; LC<sub>50</sub>: 5.4µM (Matsushima et al. 2013); LC<sub>50</sub>: 5.2µM (Messinetti et al. 2018b)) or the sea urchin *P.*  
419 *lividus* (LC<sub>50</sub>: 3.1µM (Ozlem and Hatice 2007)), but more sensitive than the vertebrate zebrafish (EC<sub>50</sub>: 25µM;  
420 LC<sub>50</sub>: 73.4µM (Tse et al. 2013)), even though all the referred EC<sub>50</sub>/LC<sub>50</sub> values are within the micromolar  
421 range. At higher dose (40µM, figure S1) BPA clearly act as an aneugen by disrupting mitotic spindle formation,  
422 as previously described in other invertebrate species like *C. elegans* (Allard and Colaiacovo 2010) and sea  
423 urchin (George et al. 2008).

424

#### 425 **4.2. Bisphenols specifically alter differentiation of the ascidian pigmented cells**

426 In addition, our study reveals that BPA exerts neurodevelopmental toxicity by disrupting the differentiation  
427 of the ascidian pigmented cells. Neurodevelopmental defects induced by BPA have been found in vertebrates  
428 (mouse, fish, frog, reviewed in Inadera 2015; Nesan, Sewell, and Kurrasch 2017) and in invertebrates such as  
429 *Drosophila* (Kaur et al. 2015), *C. elegans* (Mersha et al. 2015), *P. mammillata* (Messinetti et al. 2018a) and  
430 *Ciona robusta* (Messinetti et al. 2018b). Time-lapse live imaging of the transparent *Phallusia* embryos allowed  
431 us to describe in detail the differentiation of pigmented cells occurring in the ascidian brain (Racioppi et al.  
432 2014; Esposito et al. 2015) and how it is affected by BPA.

433 One of the main events affected by BPA was pigmentation. Several studies described pigmentation  
434 problems caused by BPA both in invertebrates and vertebrates. Concerning invertebrates, a similar phenotype  
435 was observed in another *P. mammillata* study (Messinetti et al. 2018a) and in *C. robusta* (Messinetti et al.  
436 2018b), where both ocellus and otolith were severely affect by BPA, either characterized by reduced,  
437 supernumerary or a total absence of pigmented cells. In vertebrates, the pigmentation process consists in the  
438 production of melanin pigments and later storage in melanosomes. Pigmentation in vertebrates is mostly  
439 regulated by microphthalmia-associated transcription factor (MITF) and dependent on proteins such as  
440 tyrosinase (Tyr), tyrosinase-related proteins (Tyrrp) and Rab GTPases (Wasmeier et al. 2008). In *Ciona*, PC  
441 specification is also dependent on Mitf, Tyr, Tyrrp and Rab32/38 (Abitua et al. 2012; Racioppi et al. 2014),  
442 regulated under several FGF/MAPK signals from stage 13 up to stage 16 (Racioppi et al. 2014). In our study,  
443 the window of action of BPA (i.e. after stage 20) is after the final FGF-mediated induction of PC lineage (at  
444 stage 16), suggesting that BPA is affecting PC differentiation rather than PC specification. Several  
445 observations confirmed that PC specification is not affected by BPA. First, inhibiting PC specification by timed  
446 inhibition of MAPK signaling (using UO126) did not phenocopy BPA phenotype. Second, several marker  
447 genes for PC and CNS specification in ascidians (Tyr, Rab32/38, Pax6, Cnga, Coe and Islet) are not affected  
448 by BPA exposure. Altogether, our data reinforces the idea that BPA is not acting at the PC specification level,  
449 but most likely during PC differentiation. However, the gene regulatory networks involved in ascidian PC  
450 differentiation are not known and thus more efforts are needed to assess the potential genes that are being  
451 affected by BPA.

452 The otolith movement within the sensory vesicle was another clear effect after BPA exposure, resulting in a  
453 shorter distance between the ocellus and the otolith. By imaging transgenic *Phallusia* embryos expressing  
454 GFP markers in the PC lineage (*Tyrrp*, *βCrystallin* and *Msx*), it was possible to visualize that the otolith cell  
455 changes shape and protrudes into the sensory vesicle lumen, which is enclosed by the sensory vesicle  
456 epithelium. The otolith cell assumes a round shape at the beginning of PC differentiation, and then becomes a  
457 pigmented cup-shaped cell with a foot that moves towards the ventral side of the sensory vesicle, while the  
458 ocellus remains embedded in the dorsal sensory vesicle epithelium. BPA did not inhibit foot formation but did  
459 prevent the detachment of the otolith from the dorsal sensory vesicle epithelium. Our data also suggests that  
460 the lower PC distance observed in BPA-treated embryos may also be due to a reduced expansion of the  
461 sensory vesicle lumen. Indeed, even though it was not quantified, we noticed that all bisphenols and ERR

462 antagonists also reduced the size of the sensory vesicle lumen. Because the ocellus and the otolith are  
463 located on opposite sides of the sensory vesicle, lumen expansion should participate in the separation of the  
464 two cells from each other. It has been shown that the ammonium transporter AMT-1a (Marino et al. 2007) and  
465 the ions transporter SLC26a (Deng et al. 2013) proteins are involved in sensory vesicle lumen expansion in  
466 ascidians. It would be thus interesting to assess if such genes are affected by BPA.

467 Strikingly, exposure of ascidian embryos to the BPA analogues BPE and BPF also inhibited pigmentation  
468 and the otolith movement towards the ventral side of the sensory vesicle. Such otolith phenotype seems to be  
469 specific to bisphenols since exposure to the bisphenyl 2,2DPP had no effect on larvae sensory vesicle (neither  
470 pigmentation, neither otolith movement nor sensory vesicle lumen). Interestingly, in zebrafish more than 50%  
471 of the embryos exposed to 25  $\mu$ M BPA displayed abnormal otoliths (Gibert et al. 2011), with a similar  
472 bisphenol-specificity effect (Tohmé et al. 2014), suggesting that, even if zebrafish and ascidian otoliths as  
473 structurally different, bisphenols may share a similar mode of action in both ascidians and fish,. Because BPA,  
474 BPE and BPF can bind ERR and not 2,2 DDP (due to the lack of hydroxyl groups on its phenyl rings (Okada et  
475 al. 2008; Starovoytov et al. 2014)), our data indicate that, like in zebrafish (Tohmé et al. 2014), BPA may  
476 impair otolith development by affecting ERR activity.

#### 477 478 **4.3. BPA may target ERR during otolith movement in ascidian larvae**

479 Recent evidence demonstrates that BPA is a weak ligand for the estrogen receptor (ER) but high affinity  
480 ligand for the estrogen-related receptor gamma (ERR $\gamma$ ) (Liu et al. 2014). This possibility was explored in the  
481 ascidian embryo. Ascidian genome have only one gene coding for ERR, and no estrogen nor steroid receptors  
482 (Yagi et al. 2003).

483 Transcriptomic data indicates ERR expression only at stage 26 for *Ciona robusta* and *Phallusia mammillata*  
484 (*Aniseed* database). In other ascidian species, PCR analysis showed that in *Herdmania curvata* ERR is  
485 expressed from gastrula (st. 10) throughout development (Devine et al. 2002), while *Halocynthia roretzi* ERR  
486 is expressed only from eggs up to gastrula (Park et al. 2009). Transcriptomic data available for *C. robusta* and  
487 *P. mammillata* ERR and our present data about *P. mammillata* ERR are not in agreement with the referred  
488 studies, as we show here that ERR transcripts and protein are present only from larvae (st. 26). Strikingly, we  
489 found that *Pm*-ERR is expressed within the sensory vesicle, specifically around the PC, around the time when  
490 the otolith moves towards the ventral side of the sensory vesicle. Additionally, most of the aminoacids known  
491 to be crucial for BPA specific binding to human ERR $\gamma$  (Takayanagi et al. 2006; Okada et al. 2008; Liu et al.  
492 2014) are conserved in *Pm*-ERR (data not shown), further supporting the hypothesis that BPA might bind to  
493 *Pm*-ERR to impair PC differentiation.

494 Our pharmacological screen suggests that ERR may be involved in the effect of BPA on the ascidian otolith  
495 movement. Firstly, lack of effect with the vertebrate ER agonist  $\beta$ -Estradiol 3-benzoate (E2B) is consistent with  
496 the fact that no ER-like or GPER-like proteins can be found in the ascidian genome (Yagi et al. 2003; Kamesh  
497 et al. 2008). Secondly, ERR antagonists diethylstilbestrol (DES) and 4-hydroxytamoxifen (4OHT) significantly  
498 reduced the distance between the two pigmented cells, suggesting a blocked otolith movement just as with  
499 BPA. Moreover, DES and 4OHT were able to suppress *Halocynthia roretzi* ERR activity in a dose-dependent  
500 manner (Park et al. 2009). However, it is important to point out that our data is different from a recent study  
501 (Messinetti et al. 2018a). While we found that the BPA phenotype is recapitulated by ERR inhibition using two  
502 different ERR antagonists (DES and 4OHT), Messinetti and colleagues found that an ERR antagonist (4OHT)  
503 could partially rescue the phenotype induced by BPA. Such difference may lie in the different criteria used to  
504 select embryonic cultures (>80% normal embryos and >300  $\mu$ m<sup>2</sup> PC area in our study). Thus, our study  
505 suggests that BPA targets *Pm*-ERR to block otolith movement within the ascidian sensory vesicle.

#### 506 507 **4.4. BPA pleiotropic action in ascidian larvae**

508 Finally, even if ERR is involved, it is probably not the only target in ascidian larvae. As mentioned before,  
509 exposure of ascidian embryos to vertebrate ERR antagonists inhibited otolith movement in a similar way to  
510 BPA, but it did not reduce pigmentation as reported after BPA exposure. The effect of BPA on pigmentation  
511 may be attributed to a partial inhibition of tyrosinase enzymatic activity, as bisphenols can inhibit tyrosinase  
512 enzymatic activity (Ruzza et al. 2017). Nevertheless, complete inhibition of tyrosinase enzyme by PTU  
513 resulted in larvae with well-formed pigmented cells but no melanin inside their melanosomes (Dumollard,

514 Gomes personal observations), a phenotype that was never observed with BPA, even at higher doses.  
515 Therefore, we hypothesize that BPA affects ERR and may also partially affects tyrosinase activity.

516 In addition, it is also important to note that BPA is affecting the otolith movement (PC distance) twice  
517 stronger than vertebrate ERR antagonists (31% vs ~60%), suggesting that BPA may have a pleiotropic action  
518 by targeting other nuclear receptors. Indeed, vertebrate Pregnane X Receptor (PXR), Thyroid Receptor (TR)  
519 and Peroxisome Proliferator-Activated Receptor (PPAR) have been shown to bind BPA (Moriyama et al. 2002;  
520 Sui et al. 2012; Delfosse et al. 2014; Ahmed and Atlas 2016) and ascidian orthologs are expressed in or near  
521 the larval brain during PC development (Gomes et al. 2019). Furthermore, ascidian PXR/VDR $\alpha$  has been  
522 shown to bind BPA (*Ciona robusta*, K<sub>d</sub>: 5  $\mu$ M) (Richter and Fidler, 2015). Receptor-ligand assays testing  
523 different ascidian NRs would be of greatest interest to characterize more in detail the multiple targets of BPA  
524 in ascidians that support its neurodevelopmental toxicity.

525

## 526 **5. Conclusion**

527 In this manuscript we show that BPA affects pigmentation and otolith movement in the brain of an  
528 invertebrate chordate species, the ascidian *Phallusia mammillata*. Because pigmented cells are part of the  
529 brain of the ascidian larvae, we demonstrate here that BPA induces neurodevelopmental toxicity to *P.*  
530 *mammillata* embryos.

531 We describe here for the first time the otolith formation and its movement towards the ventral side of the  
532 ascidian sensory vesicle. The expression of the nuclear receptor ERR during PC development, as well as the  
533 pharmacological approach, supports the hypothesis that ERR is involved in BPA neurodevelopmental toxicity,  
534 i.e., *Pm*-ERR may be involved in the otolith movement within the sensory vesicle. Because ERR antagonists  
535 did not affect the pigmentation process, the reduction of pigmentation induced by BPA is most likely controlled  
536 by other pathways. The potential binding of BPA to *P. mammillata* ERR, as well as the involvement of other  
537 nuclear receptors (PPAR, PXR and TR) in BPA neurodevelopmental toxicity is now being investigated in our  
538 laboratory.

539

## 540 **Supplementary data**

541 Supplementary figures are provided after the manuscript. Supplementary videos can be visualized from the  
542 following link: <https://omero.france-bioinformatique.fr/omero/webclient/?show=dataset-2177>

543

## 544 **Acknowledgements**

545 The authors would like to thank Filomena Ristoratore and Alberto Stolfi for kindly providing ascidian  
546 tyrosinase-related protein and  $\beta$ Crystallin promoters, respectively. Furthermore, the authors would like to  
547 thank Laurent Gilletta and Régis Lasbleiz and the *Centre de Ressources Biologiques Marines* of the *Institut de*  
548 *la Mer de Villefranche (CRBM - IMEV)* that is supported by *EMBRC-France*, whose French state funds are  
549 managed by the *Agence Nationale de la Recherche (ANR)* within the “*Investissement d’Avenir*” program  
550 (ANR-10-INBS-02). The experiments reported in this study were financed by an ANR grant (*Marine-*  
551 *EmbryoTox* project, ANR-14-OHRI-0009-01-1). Ievgeniia Gazo thanks to the Ministry of Education, Youth and  
552 Sports of the Czech Republic and projects CENAKVA (LM2018099) and Reproductive and Genetic  
553 Procedures for Preserving Fish Biodiversity and Aquaculture (CZ.02.1.01/0.0/0.0/16\_025/0007370).

554

## 555 **Competing interests**

556 The authors have no competing interest to declare.

557

## 558 **References**

- 559 Abitua PB, Wagner E, Navarrete IA, Levine M. 2012. Identification of a rudimentary neural crest in a non-  
560 vertebrate chordate. Whitacre DM, editor. *Nature*. 492:104–108.  
561 doi:10.1016/j.biotechadv.2011.08.021.Secreted.
- 562 Acconcia F, Pallottini V, Marino M. 2015. Molecular mechanisms of action of BPA. *Dose-Response*. 13(4):1–9.  
563 doi:10.1177/1559325815610582.
- 564 Ahmed S, Atlas E. 2016. Bisphenol S- and bisphenol A-induced adipogenesis of murine preadipocytes occurs  
565 through direct peroxisome proliferator-activated receptor gamma activation. *Int J Obes*. 40(10):1566–1573.  
566 doi:10.1038/ijo.2016.95.

567 Allard P, Colaiacovo MP. 2010. Bisphenol A impairs the double-strand break repair machinery in the germline  
568 and causes chromosome abnormalities. *Proc Natl Acad Sci.* 107(47):20405–20410.  
569 doi:10.1073/pnas.1010386107.

570 Braun JM. 2017. Early-life exposure to EDCs: Role in childhood obesity and neurodevelopment. *Nat Rev*  
571 *Endocrinol.* 13(3):161–173. doi:10.1038/nrendo.2016.186.

572 Canesi L, Fabbri E. 2015. Environmental effects of BPA: Focus on aquatic species. *Dose-Response.* 13(3).  
573 doi:10.1177/1559325815598304.

574 Caracciolo A, Gesualdo I, Branno M, Aniello F, Di Lauro R, Palumbo A. 1997. Specific cellular localization of  
575 tyrosinase mRNA during *Ciona intestinalis* larval development. *Dev Growth Differ.* 39:437–444.

576 Delfosse V, Grimaldi M, le Maire A, Bourguet W, Balaguer P. 2014. Nuclear Receptor Profiling of Bisphenol-A  
577 and Its Halogenated Analogues. 1st ed. Elsevier Inc.

578 Deng W, Nies F, Feuer A, Bo I. 2013. Anion translocation through an Slc26 transporter mediates lumen  
579 expansion during tubulogenesis. doi:10.1073/pnas.1220884110/-  
580 /DCSupplemental.www.pnas.org/cgi/doi/10.1073/pnas.1220884110.

581 Devine C, Hinman VF, Degnan BM. 2002. Evolution and developmental expression of nuclear receptor genes  
582 in the ascidian *Herdmania*. *Int J Dev Biol.* 46:687–692.

583 Dilly N. 1962. Studies on the receptors in the cerebral vesicle of the ascidian tadpole: 1. The otolith. *Q J*  
584 *Microsc Sci.* 103(3):393–398. doi:10.1007/BF00321477.

585 Dilly N. 1964. Studies on the receptors in the cerebral vesicle of the ascidian tadpole: 2. The ocellus. *Q J*  
586 *Microsc Sci.* 105(1):13–20. doi:10.1007/BF00321477.

587 Dumollard R, Gazo I, Gomes IDL, Besnardeau L, McDougall A. 2017. Ascidiaceae: An Emerging Marine Model  
588 for Drug Discovery and Screening. *Curr Top Med Chem.* 17:1–15. doi:10.2174/1568026617666170130.

589 Esposito R, Racioppi C, Pezzotti MR, Branno M, Locascio a., Ristoratore F, Spagnuolo a. 2015. The ascidian  
590 pigmented sensory organs: structures and developmental programs. *Genesis.* 53(November 2014):15–33.  
591 doi:10.1002/dvg.22836.

592 Flint S, Markle T, Thompson S, Wallace E. 2012. Bisphenol A exposure, effects, and policy: a wildlife  
593 perspective. *J Environ Manage.* 104:19–34. doi:10.1016/j.jenvman.2012.03.021. [accessed 2012 Nov 4].  
594 <http://www.ncbi.nlm.nih.gov/pubmed/22481365>.

595 George O, Bryant BK, Chinnasamy R, Corona C, Arterburn JB, Shuster CB. 2008. Bisphenol A directly targets  
596 tubulin to disrupt spindle organization in embryonic and somatic cells. *ACS Chem Biol.* 20(3):123–132.

597 Gibert Y, Sassi-Messai S, Fini J-B, Bernard L, Zalko D, Cravedi J-P, Balaguer P, Andersson-Lendahl M,  
598 Demeneix B, Laudet V. 2011. Bisphenol A induces otolith malformations during vertebrate embryogenesis.  
599 *BMC Dev Biol.* 11(1):4. doi:10.1186/1471-213X-11-4.

600 Heyer DB, Meredith RM. 2017. Environmental toxicology: Sensitive periods of development and  
601 neurodevelopmental disorders. *Neurotoxicology.* 58:23–41. doi:10.1016/j.neuro.2016.10.017.

602 Holzer G, Markov G V., Laudet V. 2017. Evolution of Nuclear Receptors and Ligand Signaling: Toward a Soft  
603 Key–Lock Model? 1st ed. Elsevier Inc.

604 Hotta K, Mitsuhashi K, Takahashi H, Inaba K, Oka K, Gojobori T, Ikeo K. 2007. A web-based interactive  
605 developmental table for the Ascidian *Ciona intestinalis*, including 3D real-image embryo reconstructions: I.  
606 From fertilized egg to hatching larva. *Dev Dyn.* 236:1790–1805. doi:10.1002/dvdy.21188.

607 Hudson C. 2016. The central nervous system of ascidian larvae. *WIREs Dev Biol.* doi:10.1002/wdev.239.

608 Hunt PA, Koehler KE, Susiarjo M, Hodges CA, Ilagan A, Voigt RC, Thomas S, Thomas BF, Hassold TJ. 2003.  
609 Bisphenol A Exposure Causes Meiotic Aneuploidy in the Female Mouse. *Curr Biol.* 13:546–553.  
610 doi:10.1016/S.

611 Inadera H. 2015. Neurological effects of bisphenol A and its analogues. *Int J Med Sci.* 12(12):926–936.  
612 doi:10.7150/ijms.13267.

613 Kamesh N, Aradhyam GK, Manoj N. 2008. The repertoire of G protein-coupled receptors in the sea squirt  
614 *Ciona intestinalis*. *BMC Evol Biol.* 8(129):1–19. doi:10.1186/1471-2148-8-129.

615 Kaur K, Simon A, Chauhan V, Chauhan A. 2015. Effect of bisphenol A on *Drosophila melanogaster* behavior –

- 616 A new model for the studies on neurodevelopmental disorders. *Behav Brain Res.* 284:77–84.  
617 doi:10.1016/j.bbr.2015.02.001.
- 618 Konno A, Kaizu M, Hotta K, Horie T, Sasakura Y, Ikeo K, Inaba K. 2010. Distribution and structural diversity of  
619 cilia in tadpole larvae of the ascidian *Ciona intestinalis*. *Dev Biol.* 337(1):42–62.  
620 doi:10.1016/j.ydbio.2009.10.012.
- 621 Krishnan A V, Stathis P, Permuth SF, Tokes L, Feldman D. 1993. Bisphenol-A: an estrogenic substance is  
622 released from polycarbonate flasks during autoclaving. *Endocrinology.* 132(6):2279–2286.
- 623 Liu X, Matsushima A, Shimohigashi M, Shimohigashi Y. 2014. A characteristic back support structure in the  
624 bisphenol A-binding pocket in the human nuclear receptor ERR $\gamma$ . *PLoS One.* 9(6).  
625 doi:10.1371/journal.pone.0101252.
- 626 Mackay H, Abizaid A. 2018. A plurality of molecular targets: The receptor ecosystem for bisphenol-A (BPA).  
627 *Horm Behav.* 101:59–67. doi:10.1016/j.yhbeh.2017.11.001.
- 628 Marino R, Melillo D, Filippo MDI, Yamada A, Pinto MR, Santis RDE, Brown ER, Matassi G. 2007. Ammonium  
629 Channel Expression Is Essential for Brain Development and Function in the Larva of *Ciona intestinalis*. *J*  
630 *Comp Neurol.* 503:135–147. doi:10.1002/cne.
- 631 Markov G V., Laudet V. 2011. Origin and evolution of the ligand-binding ability of nuclear receptors. *Mol Cell*  
632 *Endocrinol.* 334(1–2):21–30. doi:10.1016/j.mce.2010.10.017.
- 633 Matsushima A, Ryan K, Shimohigashi Y, Meinertzhagen I a. 2013. An endocrine disruptor, bisphenol A,  
634 affects development in the protochordate *Ciona intestinalis*: Hatching rates and swimming behavior alter in a  
635 dose-dependent manner. *Environ Pollut.* 173:257–263. doi:10.1016/j.envpol.2012.10.015.
- 636 McDougall A, Chenevert J, Pruliere G, Costache V, Hebras C, Salez G, Dumollard R. 2015. Centrosomes and  
637 spindles in ascidian embryos and eggs. Elsevier.
- 638 Mersha MD, Patel BM, Patel D, Richardson BN, Dhillon HS. 2015. Effects of BPA and BPS exposure limited to  
639 early embryogenesis persist to impair non-associative learning in adults. *Behav Brain Funct.* 11(27):1–5.  
640 doi:10.1186/s12993-015-0071-y.
- 641 Messinetti S, Mercurio S, Pennati R. 2018a. Effects of bisphenol A on the development of pigmented organs in  
642 the ascidian *Phallusia mammillata*. *Invertebr Biol.*(September):1–10. doi:10.1111/ivb.12231.
- 643 Messinetti S, Mercurio S, Pennati R. 2018b. Bisphenol A affects neural development of the ascidian *Ciona*  
644 *robusta*. *J Exp Zool Part A Ecol Integr Physiol.*(August):1–12. doi:10.1002/jez.2230.
- 645 Moriyama K, Tagami T, Akamizu T, Usui T, Saijo M, Kanamoto N, Hataya Y, Shimatsu A, Kuzuya H, Nakao K.  
646 2002. Thyroid hormone action is disrupted by bisphenol A as an antagonist. *J Clin Endocrinol Metab.*  
647 87(11):5185–5190. doi:10.1210/jc.2002-020209.
- 648 Murata M, Kang J. 2017. Bisphenol A ( BPA ) and cell signaling pathways. *Biotechnol Adv.*(August):0–1.  
649 doi:10.1016/j.biotechadv.2017.12.002.
- 650 Mustieles V, Perez-Lobato R, Olea N, Fernandez MF. 2015. Bisphenol A: Human exposure and  
651 neurobehavior. *Neurotoxicology.* 49:174–184. doi:10.1016/j.neuro.2015.06.002.
- 652 Nesan D, Sewell LC, Kurrasch DM. 2017. Opening the black box of endocrine disruption of brain  
653 development: Lessons from the characterization of Bisphenol A. *Horm Behav.*:1–15.  
654 doi:10.1016/j.yhbeh.2017.12.001.
- 655 Nishida H, Satoh N. 1989. Determination and regulation in the pigment cell lineage of the ascidian embryo.  
656 *Dev Biol.* 132(2):355–67. doi:10.1016/0012-1606(89)90232-7.
- 657 Okada H, Tokunaga T, Liu X, Takayanagi S, Matsushima A, Shimohigashi Y. 2008. Direct evidence revealing  
658 structural elements essential for the high binding ability of bisphenol a to human estrogen-related receptor  
659 gamma. *Environ Health Perspect.* 116(1):32–38. doi:10.1289/ehp.10587.
- 660 Ozlem çakal A, Hatice P. 2007. Effects of Bisphenol A on the Embryonic Development of Sea Urchin  
661 (*Paracentrotus lividus*). *Environ Toxicol.* 23:387–392. doi:10.1002/tox.
- 662 Paix A, Yamada L, Dru P, Lecordier H, Pruliere G, Chenevert J, Satoh N, Sardet C. 2009. Cortical anchorages  
663 and cell type segregations of maternal postplasmic/PEM RNAs in ascidians. *Dev Biol.* 336(1):96–111.  
664 doi:10.1016/j.ydbio.2009.09.001.
- 665 Park W, Kim GJ, Choi HS, Vanacker JM, Sohn YC. 2009. Conserved properties of a urochordate estrogen

- 666 receptor-related receptor (ERR) with mammalian ERRalpha. *Biochim Biophys Acta*. 1789(2):125–134.  
667 doi:10.1016/j.bbagr.2008.08.011.
- 668 Racioppi C, Kamal AK, Razy-Krajka F, Gambardella G, Zanetti L, di Bernardo D, Sanges R, Christiaen L a.,  
669 Ristoratore F. 2014. Fibroblast growth factor signalling controls nervous system patterning and pigment cell  
670 formation in *Ciona intestinalis*. *Nat Commun*. 5:4830. doi:10.1038/ncomms5830.
- 671 Ruzza P, Serra PA, Fabbri D, Dettori MA, Rocchitta G, Delogu G. 2017. Hydroxylated biphenyls as tyrosinase  
672 inhibitor: A spectrophotometric and electrochemical study. *Eur J Med Chem*. 126:1034–1038.  
673 doi:10.1016/j.ejmech.2016.12.028.
- 674 Ryan K, Lu Z, Meinertzhagen IA. 2016. The CNS connectome of a tadpole larva of *Ciona intestinalis* (L.)  
675 highlights sidedness in the brain of a chordate sibling. *Elife*. 5:1–34. doi:10.7554/eLife.16962.
- 676 Sakurai D, Goda M, Kohmura Y, Horie T, Iwamoto H, Ohtsuki H, Tsuda M. 2004. The role of pigment cells in  
677 the brain of ascidian larva. *J Comp Neurol*. 475(1):70–82. doi:10.1002/cne.20142.
- 678 Sardet C, McDougall A, Yasuo H, Chenevert J, Pruliere G, Dumollard R, Hudson C, Hebras C, Nguyen N Le,  
679 Paix A. 2011. Embryological Methods in Ascidians: The Villefranche-sur-Mer Protocols. In: *Vertebrate  
680 Embryogenesis, Methods in Molecular Biology*. Vol. 770. p. 365–400.
- 681 Schug T, Johnson AF, Birnbaum LS, Colborn T, Guillette LJ, Crews DP, Collins T, Soto AM, vom Saal FS,  
682 McLachlan JA, et al. 2016. Endocrine Disruptors: Past Lessons and Future Directions. *Mol Endocrinol*.  
683 30(8):833–847. doi:10.1210/me.2016-1096.
- 684 Starovoytov ON, Liu Y, Tan L, Yang S. 2014. Effects of the Hydroxyl Group on Phenyl Based Ligand/ERRγ  
685 Protein Binding. *Chem Res Toxicol*. 27:1371–1379.
- 686 Stolfi A, Christiaen L. 2012. Genetic and genomic toolbox of the Chordate *Ciona intestinalis*. *Genetics*.  
687 192(1):55–66. doi:10.1534/genetics.112.140590.
- 688 Sui Y, Ai N, Park SH, Rios-Pilier J, Perkins JT, Welsh WJ, Zhou C. 2012. Bisphenol A and its analogues  
689 activate human pregnane X receptor. *Environ Health Perspect*. 120(3):399–405. doi:10.1289/ehp.1104426.
- 690 Takayanagi S, Tokunaga T, Liu X, Okada H, Matsushima A, Shimohigashi Y. 2006. Endocrine disruptor  
691 bisphenol A strongly binds to human estrogen-related receptor gamma (ERRγ) with high constitutive activity.  
692 *Toxicol Lett*. 167(2):95–105. doi:10.1016/j.toxlet.2006.08.012.
- 693 Tohmé M, Prud'Homme SM, Boulahtouf A, Samarut E, Brunet F, Bernard L, Bourguet W, Gibert Y, Balaguer  
694 P, Laudet V. 2014. Estrogen-related receptor γ is an in vivo receptor of bisphenol A. *FASEB J*. 28:3124–3133.  
695 doi:10.1096/fj.13-240465.
- 696 Tse WKF, Yeung BHY, Wan HT, Wong CKC. 2013. Early embryogenesis in zebrafish is affected by bisphenol  
697 A exposure. *Biol Open*. 2:466–71. doi:10.1242/bio.20134283.
- 698 Wasmeier C, Hume AN, Bolasco G, Seabra MC. 2008. Melanosomes at a glance. *J Cell Sci*. 121(24):3995–  
699 3999. doi:10.1242/jcs.040667.
- 700 Whittaker JR. 1966. An analysis of melanogenesis in differentiating pigment cells of ascidian embryos. *Dev  
701 Biol*. 14:1–39. doi:10.1016/0012-1606(66)90003-0.
- 702 Yagi K, Satou Y, Mazet F, Shimeld SM, Degnan B, Rokhsar D, Levine M, Kohara Y, Satoh N. 2003. A  
703 genomewide survey of developmentally relevant genes in *Ciona intestinalis*. III. Genes for Fox, ETS, nuclear  
704 receptors and NFκB. *Dev Genes Evol*. 213:235–244. doi:10.1007/s00427-003-0322-z.

705

706

707 **Figure 1. Bisphenol A is toxic to *Phallusia mammillata* embryos in a dose-dependent manner.** Embryos were  
708 exposed to different concentrations of Bisphenol A (BPA) from 1-cell stage, and three different phenotypes were assessed:  
709 *normal*, for larvae with elongated trunk and straight tail (white bars), *malformed* for larvae showing deformed trunk and/or  
710 bent tails (grey bars) and *not developed* for embryos displaying arrested development (black bars). Concentrations higher  
711 than 10 $\mu$ M significantly induced malformations. Concentrations higher than 20  $\mu$ M significantly arrested development. The  
712 median effective (EC<sub>50</sub>) and lethal (LC<sub>50</sub>) concentrations are shown.  
713

714 **Figure 2. Bisphenol A disrupts pigment cell development in *Phallusia mammillata*. (A) Timecourse of pigment cell  
715 (PC) development in non-exposed embryos.** The first pigments arrive at stage 21 (black arrowhead, t0), with an  
716 increase of pigmentation at stage 22. At stage 23, two distinct pigment cells (PC) are visible, the otolith (Ot) and the  
717 ocellus (Oc) (pink and blue arrowheads, respectively). Sensory vesicle lumen (SVL) and adhesive palps (P) (orange and  
718 yellow arrowheads, respectively) are visible as well at stage 23. Strong pigmentation for both PC is visible at stage 24. At  
719 stage 25 the trunk (T) starts to elongate (white arrowhead). Finally, at stage 26 (t5h) the trunk of the larvae is elongated  
720 and show two distinct pigmented cells, as well as adhesive palps. The otolith is now isolated within the sensory vesicle  
721 lumen. Scale bars: 10 $\mu$ m. **(B) Timecourse of PC development in Bisphenol A (BPA) exposed embryos.** Embryos were  
722 exposed to 10 $\mu$ M BPA from stage 1. Resulting BPA-exposed embryos (stage 26, t5h) showed severe reduction of  
723 pigmentation and an inhibition of otolith movement, resulting in a reduced distance between otolith and ocellus. Sensory  
724 vesicle lumen also seem reduced but it was not quantified. Trunk elongation and palps formation seem unaffected. Scale  
725 bars: 10 $\mu$ m. **(C) Effect of BPA in *P. mammillata* larvae.** Embryos were exposed to BPA 10  $\mu$ M and three endpoints were  
726 quantified: the area of both pigmented cells (PC area,  $\mu$ m<sup>2</sup>), the distance between the pigmented cells (PC distance,  $\mu$ m)  
727 and the length and width of the trunk (Trunk LW ratio). Data was normalized to the control (DMSO, 100%) and plotted in a  
728 radar chart. All the three endpoints were significantly different from the control (0.01% DMSO; ANOVA - *Dunnett's* test),  
729 with the PC area and PC distance being the most affected ones (reduced to 35% and 31%, respectively). Descriptive  
730 statistics are represented in table I. Scale bar of representative phenotype: 10 $\mu$ m. **(D) Window of sensitivity of *P.***  
731 ***mammillata* embryos to BPA.** Embryos were exposed to BPA (10 $\mu$ M): 6 hours before fertilization (6hbf, from stage 0 to  
732 1), 6 hours post fertilization (6hpf, from stage 1 to 10), before fertilization up to gastrula (from stage 0 to 10) and then at  
733 different developmental stages between stages 10 and 20. The PC area ( $\mu$ m<sup>2</sup>) was assessed at stage 26, when  
734 pigmentation process is finished. Exposure to BPA from stage 1 to 26, as well as all exposures between stage 10 and 20  
735 were significantly different from the control (0.01% DMSO; ANOVA - *Dunnett's* test; \*\*\* p-value<0,001). Each point  
736 represents one embryo (n $\geq$ 50 embryos from three independent experiments).  
737

738 **Figure 3. Bisphenol specifically disrupt otolith movement towards the ventral side of the sensory vesicle. (A)**  
739 **Pigment cells development within the sensory vesicle.** At stage 21, otolith cell (followed by  $\beta\gamma$ -*Crystallin* promoter  
740 *p $\beta\gamma$ C::GFP*) is visible within the sensory vesicle. The sensory vesicle surrounds the lumen that results from neural tube  
741 closure. At later stages (st. 23, 25), the otolith develops a foot that will allow the cell to move towards the ventral side of the  
742 brain sensory vesicle. Scale bars are 50 $\mu$ m, except insets (15 $\mu$ m). **(B) Timelapse of otolith movement towards the**  
743 **ventral side of the sensory vesicle lumen.** At the beginning of the pigmentation, otolith cell is next to ocellus cell (st. 22).  
744 Later, the epithelium invaginates towards the ventral side of the sensory vesicle lumen (st. 23-25), allowing the otolith to  
745 move away from the ocellus. At the end, the otolith foot is ventral and pigments are dorsal within the otolith cell (st. 26).  
746 Scale bars: 10 $\mu$ m. **(C) Timelapse of otolith movement in the presence of BPA.** In BPA-exposed embryos (BPA 10 $\mu$ M),  
747 otolith cell is next to ocellus cell (st. 22) and the epithelium still invaginates (st. 23-25), however the otolith stays attached  
748 to the epithelium (st. 26) until the embryo metamorphoses (not shown). Besides reduced pigmentation and blocked otolith  
749 movement, the sensory vesicle lumen seems reduced as well when compared to the control. Scale bars: 10 $\mu$ m.  
750 Supplementary videos 1 and 2 of described timelapses (B and C) can be downloaded from [http://lbdv-local.obs-  
752 vlfr.fr/~dumollard/](http://lbdv-local.obs-<br/>751 vlfr.fr/~dumollard/).

753 **Figure 4. Bisphenols, but not bisphenyl, specifically disrupt pigmentation and otolith movement towards the**  
754 **ventral side of the sensory vesicle. (A) Molecular structures of BPA, BPE, BPF and 2,2DPP. (B-F) Comparison of**  
755 **otolith foot structure between non-exposed embryos (0.01% DMSO), and bisphenols and bisphenyl.** In non-  
756 exposed larvae **(B: 0.01% DMSO)**, the otolith foot (purple dot) is attached to the ventral side of the sensory vesicle, and an  
757 accumulation of actin is observed. A similar otolith foot phenotype was also visible in larvae exposed to 2,2 DPP **(F)**.  
758 However, in larvae exposed to BPA **(C)**, BPE **(D)** and BPF **(E)**, the otolith foot is arrested on the posterior or even dorsal  
759 side of the sensory vesicle. For comparison, all larvae were exposed to 10 $\mu$ M of each drug with exception for 2,2 DPP that  
760 showed no otolith phenotype either at 10, 25 or 100  $\mu$ M. Larvae were fixed and stained for actin and DNA (Phalloidin and  
761 Hoechst staining, respectively). *n*: nucleus, *f*. foot, *v*. ventral. All scale bars are 50 $\mu$ m (insets: 15 $\mu$ m).  
762

763 **Figure 5. *Phallusia mammillata* express an Estrogen-Related Receptor (ERR) in the ascidian larval sensory**  
764 **vesicle. (A) *Pm*-ERR mRNA spatial expression.** *Pm*-ERR transcript was assessed by *in situ* hybridization and spatial

765 expression was only visible from stage 26. *Pm*-ERR mRNA is expressed within the sensory vesicle (SV), specifically  
766 bellow the otolith, above the ocellus and between both pigment cells, also in the palps and in the trunk ganglion (Tg) (black  
767 arrowheads). **(B) *Pm*-ERR promoter activity.** The promoter region of *Pm*-ERR, corresponding to 1.7kbp before the first  
768 ATG, was cloned into a *H2B::Venus* reporter plasmid and injected in *P. mammillata* eggs. Two types of expression were  
769 obtained: in the sensory vesicle and palps, or in the sensory vesicle and trunk ganglion (white arrowheads). **(C-D) *Pm*-**  
770 **ERR protein expression. (C)** In order to study protein expression, a *Pm*-ERR antibody was raised and validated by  
771 injecting eggs with exogenous ERR mRNA (*ERR::Venus*). **(D)** *Pm*-ERR protein expression was assessed in *P. mammillata*  
772 eggs, neurulas (st. 15), late tailbuds (st. 21) and larvae (st. 26), showing its presence only from stage 26 (N=6), in a similar  
773 way as mRNA and promoter results. Tubulin antibody was used as control. Scale bars: 50µm.  
774

775 **Figure 6. Estrogen-related receptor (ERR) antagonists partially phenocopied BPA neurodevelopmental toxicity,**  
776 **but not Estrogen Receptor (ER) agonist. (A-C) Three endpoint-radar charts for comparison between BPA and E2B,**  
777 **DES and 4OHT.** For phenotype comparison, the following endpoints were measured: the area of pigmented cells (PC  
778 area, µm<sup>2</sup>), the distance between pigmented cells (PC distance, µm) and the length and width of the trunk (Trunk L/W  
779 ratio). Graphs are normalized to the control (DMSO, 100%). Embryos exposed to the ER agonist β-estradiol 3-benzoate  
780 (**E2B, A**) had no effect on development. Embryos exposed to the ERR antagonist diethylstilbestrol (**DES, B**) and the ERR  
781 antagonist 4-hydroxytamoxifen (**4OHT, C**) severely affected PC distance, as well as mild reduction of trunk elongation  
782 (N≥3). Respective molecular structures and representative phenotype pictures are provided (scale bars: 20µm). Please  
783 refer to the table I for the descriptive statistics.  
784

785 **Figure S1. Bisphenol A induces genotoxicity at high doses.** *P. mammillata* eggs were fertilized and immediately  
786 exposed to BPA 40µM. Embryos were then fixed at the first mitosis (64min after fertilization) and stained for microtubules  
787 (anti-DM1α, green) and DNA (DAPI, blue). While most of non-exposed embryos (0.01% DMSO) showed a well-formed  
788 mitotic spindle, high dose of BPA blocked embryos to exit meiosis before mitosis, displaying both mitotic and meiotic  
789 spindles. Scale bars: 50µm.  
790

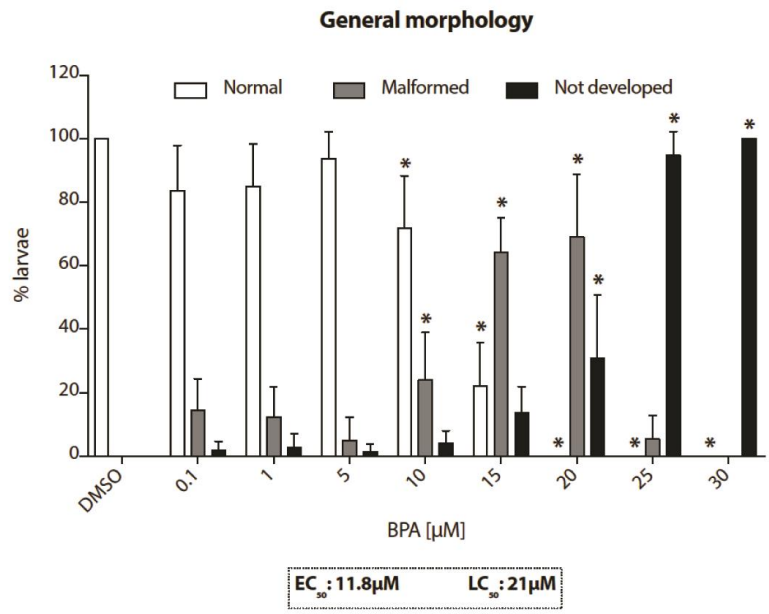
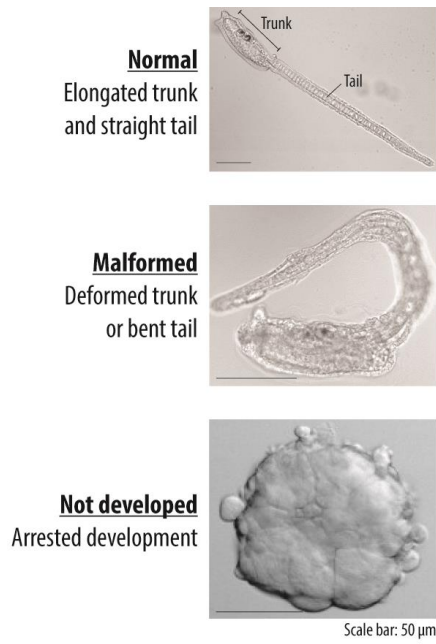
791 **Figure S2. Bisphenol A does not affect *P. mammillata* pigment cell (PC) nor central nervous system (CNS)**  
792 **specification lineages. (A) BPA phenotype is different from PTU and UO126.** Embryos were exposed to the  
793 tyrosinase enzyme inhibitor phenylthiourea (PTU, 200µM) at stage 1, and to the MAPK inhibitor UO126 (4µM) at stages 16  
794 and 18 (corresponding to before and after the last MAPK signal induction for PC specification, respectively). PTU  
795 completely abolished pigmentation (melanin) but melanosomes structures are intact. Exposure to UO126 at stage 16 also  
796 abolished pigmentation, but not when embryos were exposed to UO126 at stage 18. BPA still induced the phenotype  
797 (reduced pigmentation and otolith blocked movement) even when incubated at stage 22, but not at stage 24. Scale bars  
798 are 50µm, except insets (15µm). **(B-C) Spatial expression of PC and CNS specification genes are not affected by**  
799 **BPA.** The mRNA of genes driving/involved in **(B)** PC (*Opsin, Pax6, Rab32/38, Tyr*) and in **(C)** CNS (*Cnga, Coe, Eya, Islet*)  
800 specification were assessed by *in situ* hybridization, in both non-exposed (WT) and BPA-exposed (10µM) embryos.  
801 Expression does not seem to be affected by BPA. **(D) Cilia of the neurohypophysial duct and neural tube are not**  
802 **affected by BPA.** Expression of acetylated tubulin, marker of the ascidian neurohypophysial duct and neural tube cilia,  
803 was assessed by antibody staining, in both non-exposed (WT) and BPA-exposed (10µM) embryos. Expression does not  
804 seem to be affected by BPA. Note: all embryos were exposed to drugs from 1-cell stage, unless specified. Scale bars are  
805 50µm.  
806  
807

808 **Table I. Descriptive statistics of radar charts.** Raw data of each radar chart is provided. Data was analyzed based on  
 809 One-Way ANOVA. Because data did not follow a Gaussian distribution (normality test Shapiro-Wilk), data was analyzed  
 810 using Kruskal-Wallis test followed by Dunnett's multiple comparison test (Dunn's MCT). \* p-value<0.05; \*\* p-value<0.01;  
 811 \*\*\* p-value<0.001.  
 812

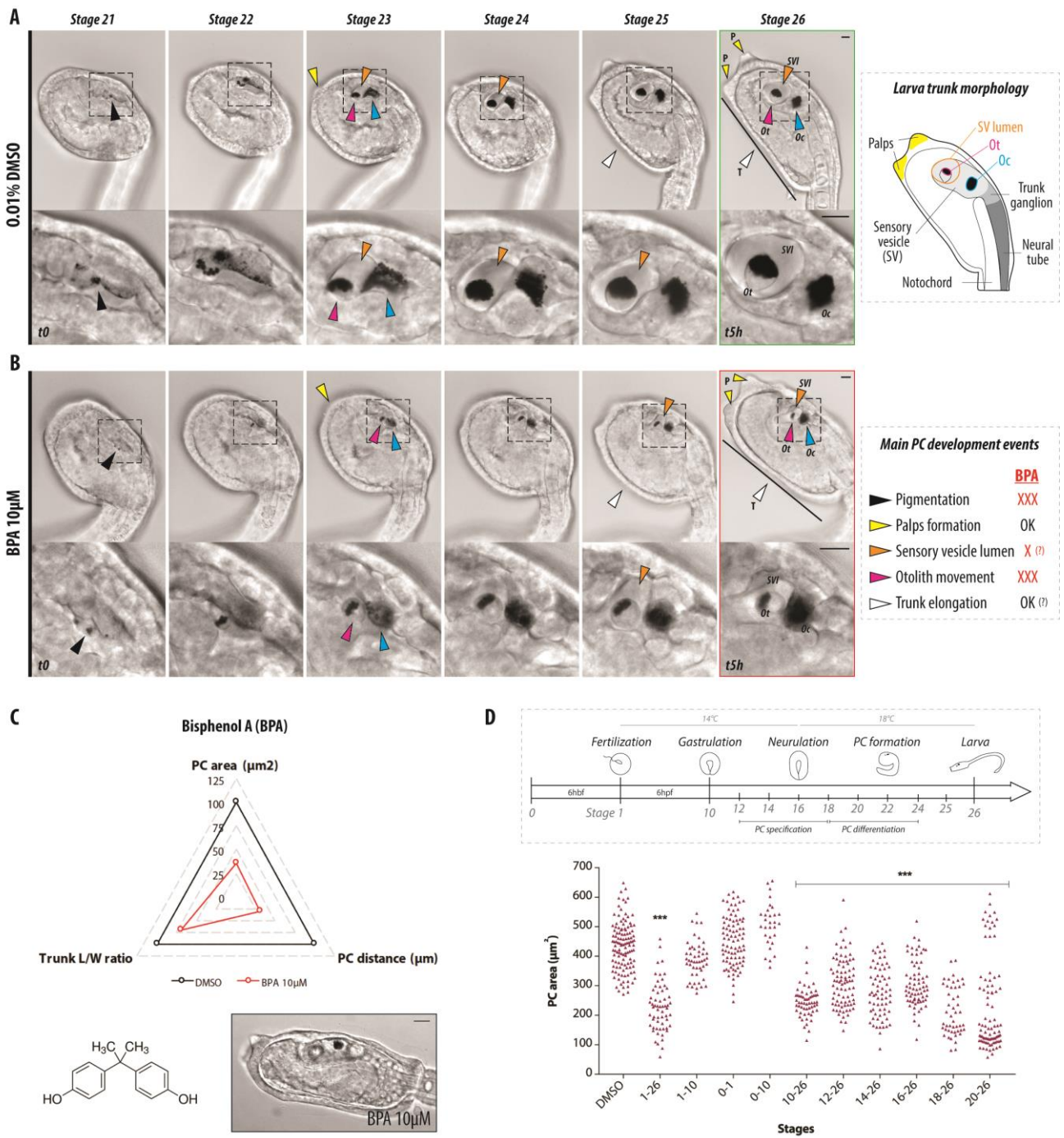
<u>PC area (µm<sup>2</sup>)</u>	n	Min	Max	Mean	Std	Dunn's MCT	% to the control	Adj p-value	Summary
DMSO	486	188	636	382	82,8	-	-	-	-
BPA 10µM	255	0	361	122	83,5	DMSO vs. BPA 10µM	35	<,001	***
E2B 10µM	162	138	602	360	100	DMSO vs. E2B 10µM	94	0,881	ns
DES 1µM	144	171	557	384	68,3	DMSO vs. DES 1µM	101	>,999	ns
4-OHT 5µM	148	73,2	624	376	102	DMSO vs. 4-OHT 5µM	98	>,999	ns
4-OHT 10µM	105	150	672	398	107	DMSO vs. 4-OHT 10µM	105	>,999	ns
<u>PC distance (µm)</u>	n	Min	Max	Mean	Std	Dunn's MCT	% to the control	Adj p-value	Summary
DMSO	485	0	41,5	24,1	8,52	-	-	-	-
BPA 10µM	278	0	32,3	7	10,1	DMSO vs. BPA 10µM	31	<,001	***
E2B 10µM	161	0	36,7	22,1	9,28	DMSO vs. E2B 10µM	88	0,15	ns
DES 1µM	145	0	34,2	15,9	11,9	DMSO vs. DES 1µM	65	<,001	***
4-OHT 5µM	149	0	40	15,3	13,1	DMSO vs. 4-OHT 5µM	63	<,001	***
4-OHT 10µM	105	0	40,6	13,9	13,6	DMSO vs. 4-OHT 10µM	58	<,001	***
<u>Trunk L/W ratio</u>	n	Min	Max	Mean	Std	Dunn's MCT	% to the control	Adj p-value	Summary
DMSO	486	1,01	4,34	2,53	0,52	-	-	-	-
BPA 10µM	279	1,01	2,89	1,72	0,41	DMSO vs. BPA 10µM	70	<,001	***
E2B 10µM	162	1,21	3,5	2,5	0,4	DMSO vs. E2B 10µM	98	>,999	ns
DES 1µM	270	1,07	2,73	1,75	0,32	DMSO vs. DES 1µM	75	<,001	***
4-OHT 5µM	148	1,36	3,82	2,29	0,53	DMSO vs. 4-OHT 5µM	91	<,001	***
4-OHT 10µM	106	1,03	2,75	1,91	0,31	DMSO vs. 4-OHT 10µM	75	<,001	***

813  
 814  
 815  
 816  
 817

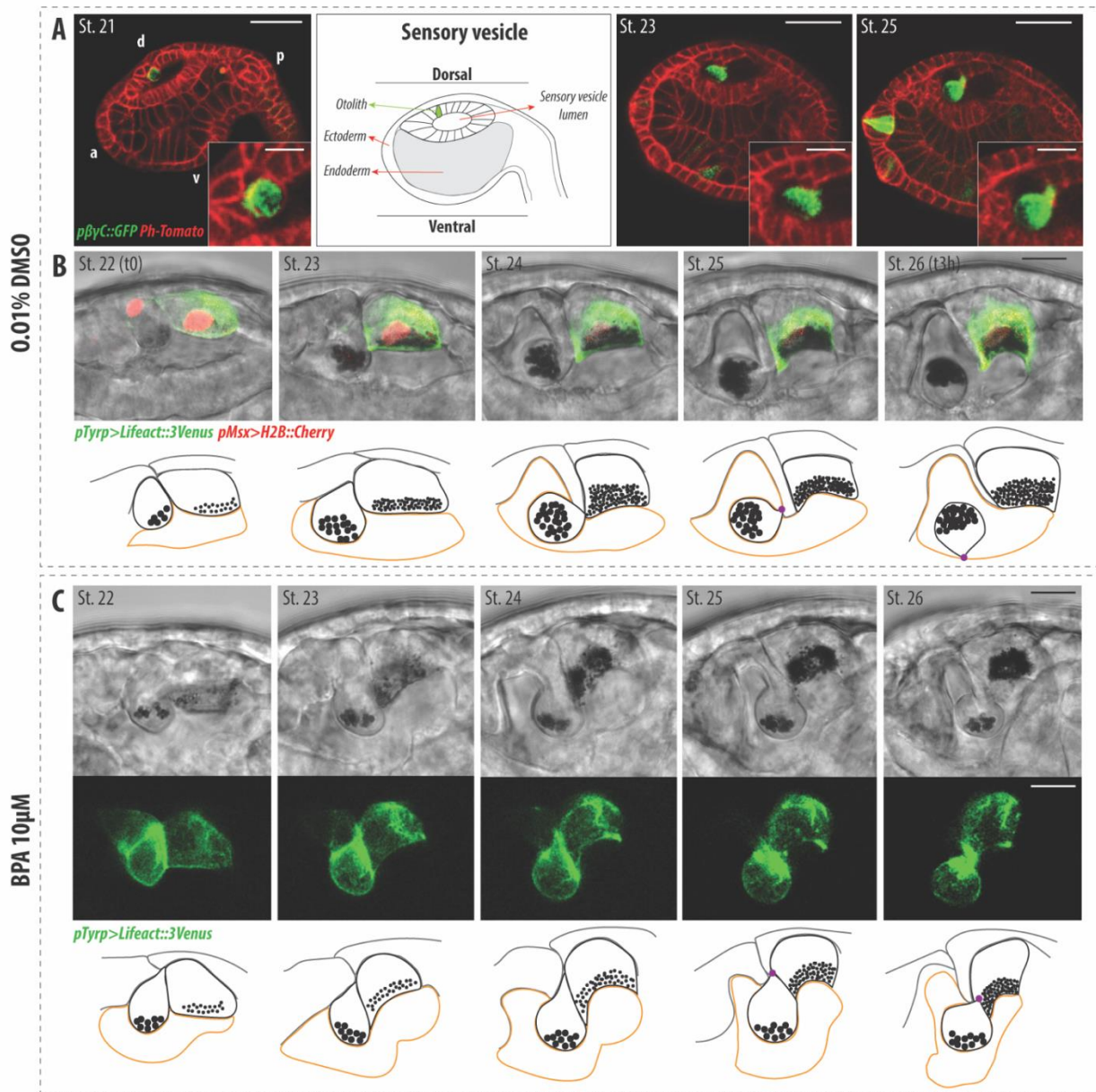
818 **Figure 1**  
 819



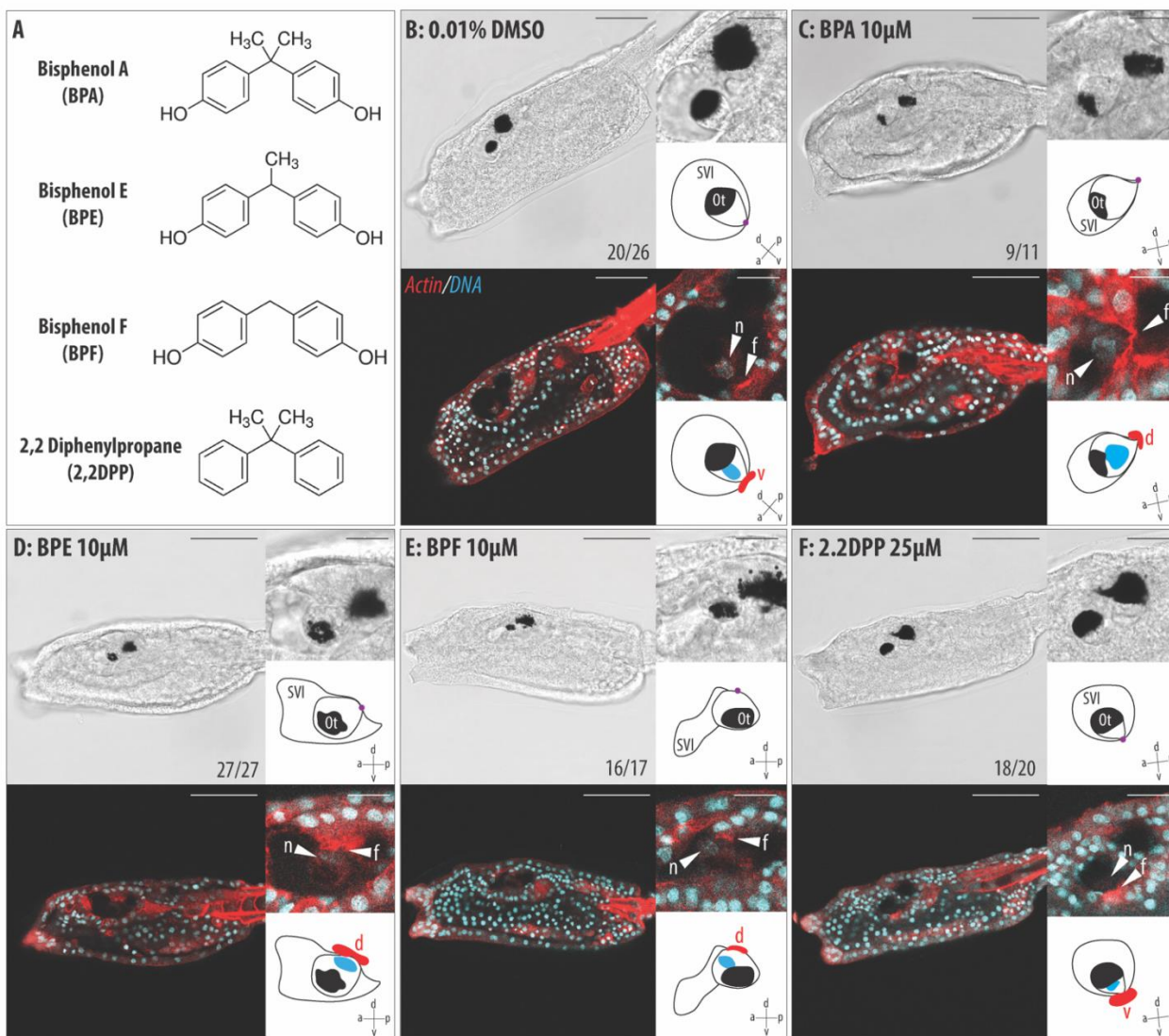
820  
 821  
 822



824  
825  
826  
827

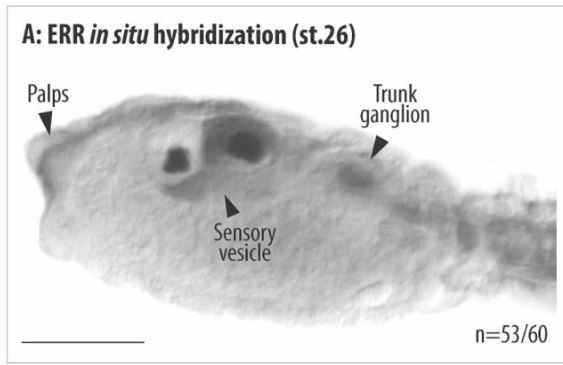


831 **Figure 4**

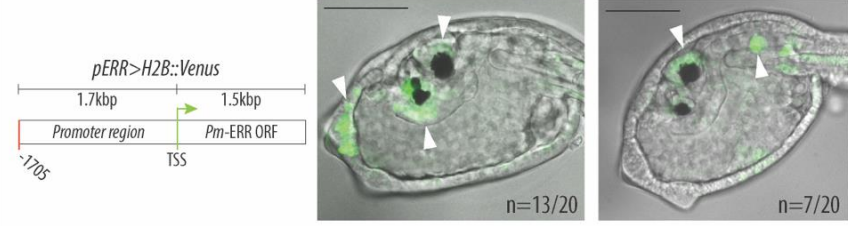


832  
 833  
 834

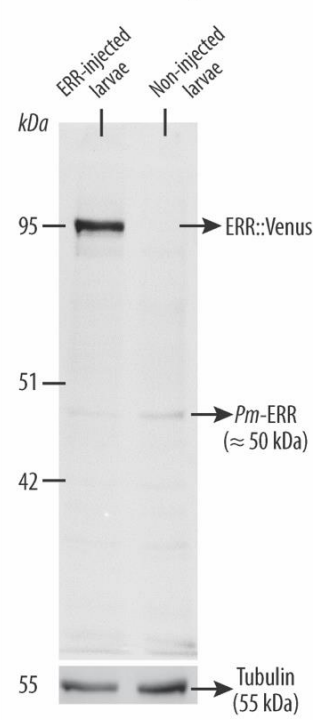
835 **Figure 5**



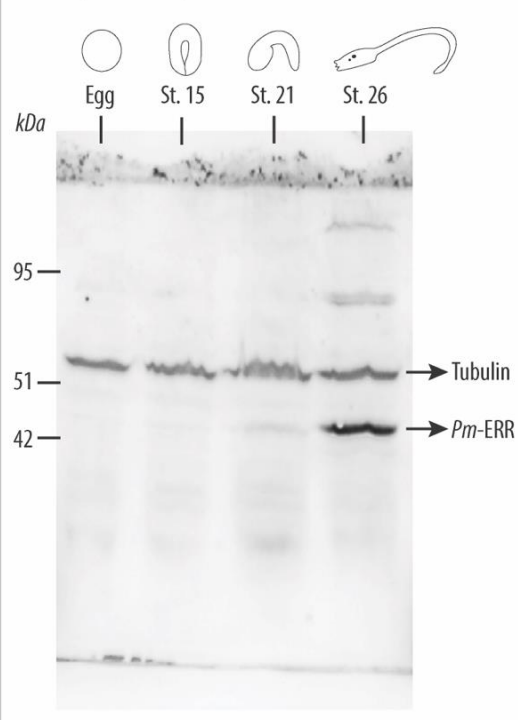
**B: ERR promoter activity**



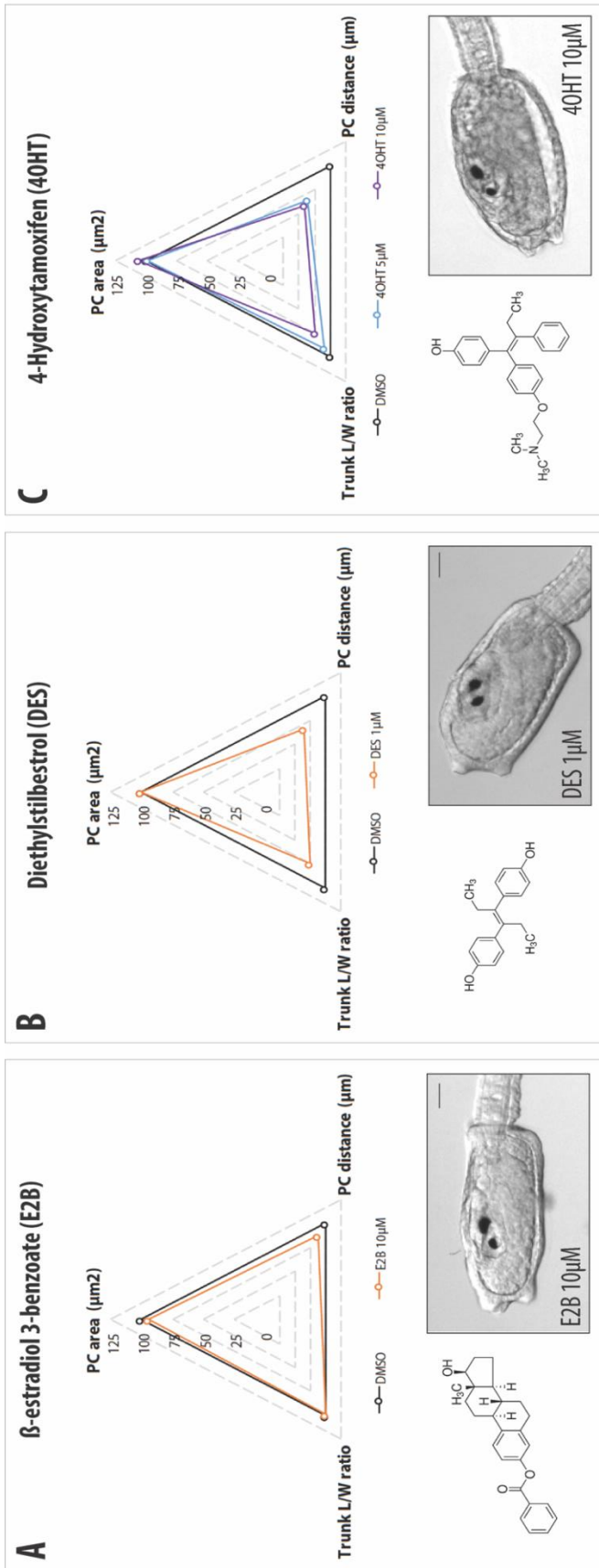
**C: Pm-ERR antibody**



**D: ERR protein expression**

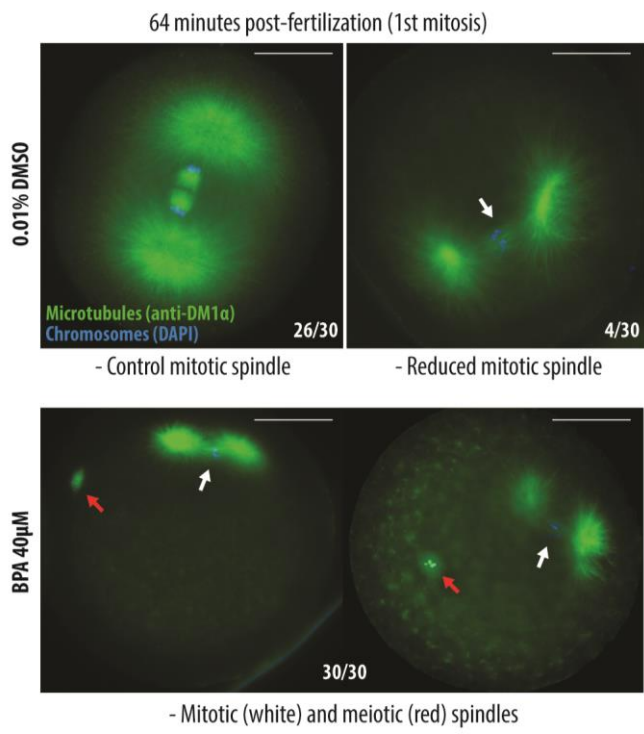


836  
837  
838



840  
841  
842

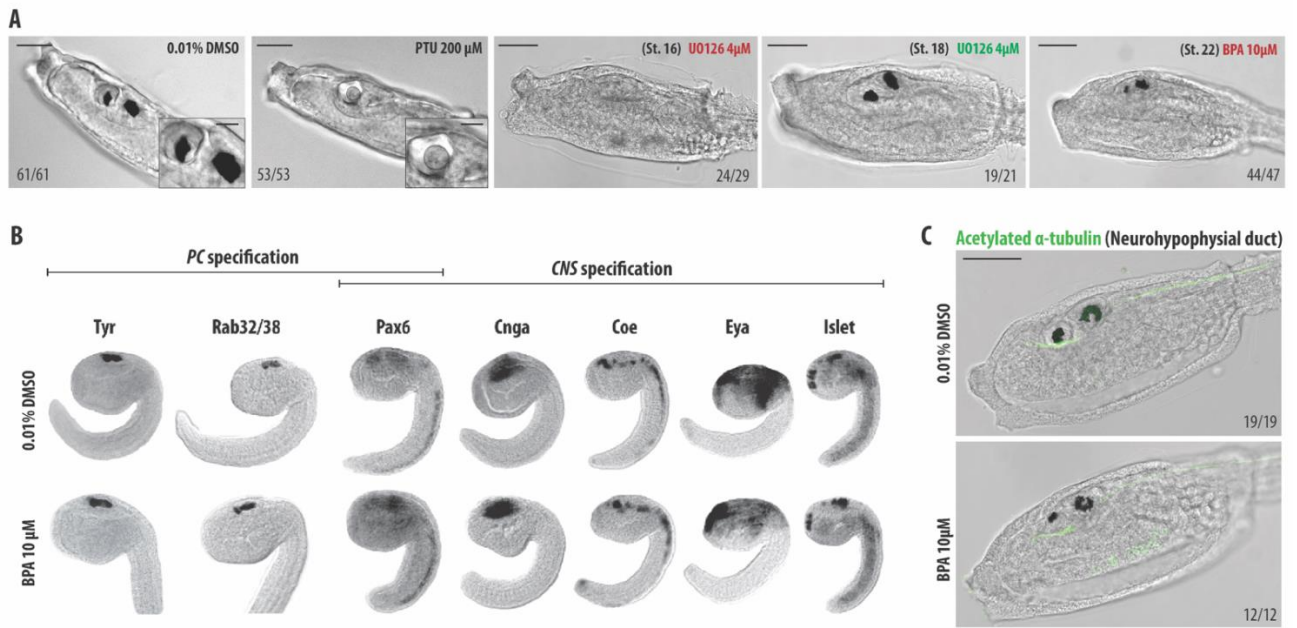
843 **Figure S1**



844  
845  
846

847  
848

Figure S2



849  
850